Incorporation of Phase Change Materials into Cementitious Systems

by

Breeann Sharma

A Thesis Presented in Partial Fulfillment
of the Requirements for the Degree
Master of Science

Approved September 2013 by the
Graduate Supervisory Committee:

Narayanan Neithalath, Chair
Subramaniam Rajan
Barzin Mobasher

ARIZONA STATE UNIVERSITY

December 2013

ABSTRACT

Manufacture of building materials requires significant energy, and as demand for these materials continues to increase, the energy requirement will as well. Offsetting this energy use will require increased focus on sustainable building materials. Further, the energy used in building, particularly in heating and air conditioning, accounts for 40 percent of a buildings energy use. Increasing the efficiency of building materials will reduce energy usage over the life time of the building. Current methods for maintaining the interior environment can be highly inefficient depending on the building materials selected. Materials such as concrete have low thermal efficiency and have a low heat capacity meaning it provides little insulation. Use of phase change materials (PCM) provides the opportunity to increase environmental efficiency of buildings by using the inherent latent heat storage as well as the increased heat capacity.

Incorporating PCM into concrete via lightweight aggregates (LWA) by direct addition is seen as a viable option for increasing the thermal storage capabilities of concrete, thereby increasing building energy efficiency. As PCM change phase from solid to liquid, heat is absorbed from the surroundings, decreasing the demand on the air conditioning systems on a hot day or vice versa on a cold day. Further these materials provide an additional insulating capacity above the value of plain concrete. When the temperature drops outside the PCM turns back into a solid and releases the energy stored from the day.

PCM is a hydrophobic material and causes reductions in compressive strength when incorporated directly into concrete, as shown in previous studies. A proposed method for mitigating this detrimental effect, while still incorporating PCM into concrete is to

encapsulate the PCM in aggregate. This technique would, in theory, allow for the use of phase change materials directly in concrete, increasing the thermal efficiency of buildings, while negating the negative effect on compressive strength of the material.

ACKNOWLEDGMENTS

I would like to express my deepest gratitude to my committee chair, Dr. Neithalath, for allowing me this opportunity to step out of my comfort zone, and guiding me through this experience. I would also like to extend my thanks to Dr. Rajan and Dr. Mobasher for being a part of my committee and teaching me structural engineering necessities.

I would like to thank my fellow research students, Amie Stockwell, Ussala Chowdhury, Matt Aguayo, Sumanta Das, Vikram Dey, Robert Kachala and Ben Rehder, in the structures department for always listening and helping whenever I had questions, specifically to Kirk Vance who showed me how to use nearly every piece of equipment, and to Akash Dakhane for assisting with experiments when I was unavailable.

This thesis is dedicated to my loving parents, George and Robyn Sharma, who have always supported me in any way they can while going through school all these years, and to my fiancé, Chris Draper, who took care of me and many of the house hold chores while I worked on this degree.

TABLE OF CONTENTS

Page

LIST OF TABLES

TABLE PAGE

LIST OF FIGURES

FIGURE PAGE

LIST OF SYMBOLS

ABBREVIATIONS

PCM	Phase Change Material
TES	Thermal Energy Storage
LWA	Lightweight aggregate
AZ	Arizona
OPC	Ordinary Portland Cement
HVAC	Heating, Ventilation and Air-Conditioning
PT	Pure Temp
SCM	Supplementary Cementious Materials
DSC	Differential Scanning Calorimetry
FTIR	Fourier Transform Infrared Spectroscopy
TGA-STA	Thermogravimetry Simultaneous Thermal Analysis
MIP	Mercury Intrusion Porosimetry
SF	Micro Silica (Silica Fume
NS	Nano Silica
w/c	Water –Cement Ratio

INTRODUCTION

The National Science and Technology Council reported that, buildings use 40% of the U.S.'s energy consumption and this will continue to grow as the population increases [1]. 40 to 50% of the energy usage in buildings is for temperature regulation [1]. Therefore, there is a substantial environmental effect from energy consumption associated with buildings, which is directly connected to carbon dioxide emissions from burning fossil fuels for power generation. Using alternative means to produce electricity is one way to reduce these emissions, but there are many limitations connected to these sources, namely that they typically are intermittent sources of power and are dependent on a location's climate or conditions. Solar energy for instance cannot be used to regulate heating and cooling in buildings at night and on particularly cloudy days because current energy storage systems are inefficient or impractical [2]. Another option to be considered along with green energy production is to adjust the thermal heat storage capabilities of building materials through sensible heat and/or latent heat storage. Sensible heat storage, as in traditional construction materials, is where heat is transferred to the material which then leads to an increase of the material temperature during the heat storage process. Latent heat storage on the other hand will absorb/release energy as it changes phase without increasing the temperature of the material until the maximum energy absorbed is achieved, after which it will behave as a sensible heat storage material.

It is estimated that 30% to 50% of energy consumption in buildings could be reduced by incorporating thermally efficient technologies into them [1]. Different technologies are available from; building materials, insulation methods, and smart systems. Engineers can

work towards the creation and implementation of new building materials and thermal systems to reduce the energy consumption of buildings.

One option is phase change materials (PCM) integration. The possible energy savings of PCM integration can be significant [3]. This thesis will explore direct incorporation of PCM into cement pastes and incorporation of PCM into lightweight aggregate (LWA) to be used in cement mortar. A study of the effects PCM has on cementitious systems, such as the pore structure, hydration and strength development will be presented in addition to the changes in the thermal characteristics and behavior of the PCM, and the PCM-cement composite.

1.1 Objective

Various studies have been completed on incorporating phase change materials into a variety of building materials including gypsum board [4, 5, 6, 7, 8, 9, 10, 11], masonry walls [12, 13]such as bricks or concrete, but the fundamental properties of these PCM in different systems is not as well understood. Incorporation into cementitious systems possesses a broader range of issues than other materials due to the non-uniform nature of concrete, and the chemical reactions associated with cement hydration, which requires further investigation. The required investigations include such items as the changes in the material properties seen in both the PCM and the cementitious systems.

The major objectives of this study are listed below:

1. To better understand the microstructural and mechanical behavior changes of cementitious systems upon incorporation of phase change materials;
2. To evaluate the thermal behavior of the phase change materials incorporated into cementitious systems;

3. Analyze impregnation of PCM into lightweight aggregate (LWA) to be used in cement and its effects on thermal and mechanical properties.

1.2 Organization of Thesis

Chapter 2 provides background on phase change materials and its applications in building materials. Previous studies utilizing PCM incorporation into concrete and cementitious systems are discussed.

Chapter 3 describes the materials utilized in this research along with the PCM incorporation methods. Mix procedures and proportions are documented in this chapter.

Chapter 4 presents the results of incorporation of PCM directly into cement pastes. Tests include differential scanning calorimetry (DSC), compression testing, isothermal calorimetry, mercury intrusion porosimetry (MIP), thermogravimetry simultaneous thermal analysis (TGA-STA), and Fourier transform infrared spectroscopy (FTIR).

Chapter 5 presents the results on PCM incorporated into LWA used in mortar mixes. Tests include differential scanning calorimetry (DSC) to determine optimal incorporation method, compression testing, isothermal calorimetry, thermal conductivity, and Fourier transform infrared spectroscopy (FTIR).

Chapter 6 summarizes the results and lists the conclusions found from this thesis. Recommended future work is also presented in this chapter.

LITERATURE REVIEW

2.1 Phase Change Materials

Phase change materials are a type of thermal energy storage material (TES); using the process of changing phase, typically a solid to liquid during a temperature range, to store latent energy, or a liquid to a solid to release stored energy [3, 14, 15, 16]. Through the phase change process the energy storage capacity of these materials is maximized while volume change associated with phase change is typically low. Latent heat, also known as phase change enthalpy and heat of fusion, is not a process most materials (such as concrete) have at ambient conditions [17]. All materials have sensible heat storage, when the material temperature increases, energy is stored in the material, but latent heat storage occurs during phase change, where the melting temperature is held constant during energy storage [1]. Figure 1-1 represents the process of latent heat storage. The PCM begins to melt as it nears its phase change temperature; it absorbs heat and stores it until the material transitions back to solid state when the stored energy is then released into the environment. These benefits make PCM very promising to be used in building systems.

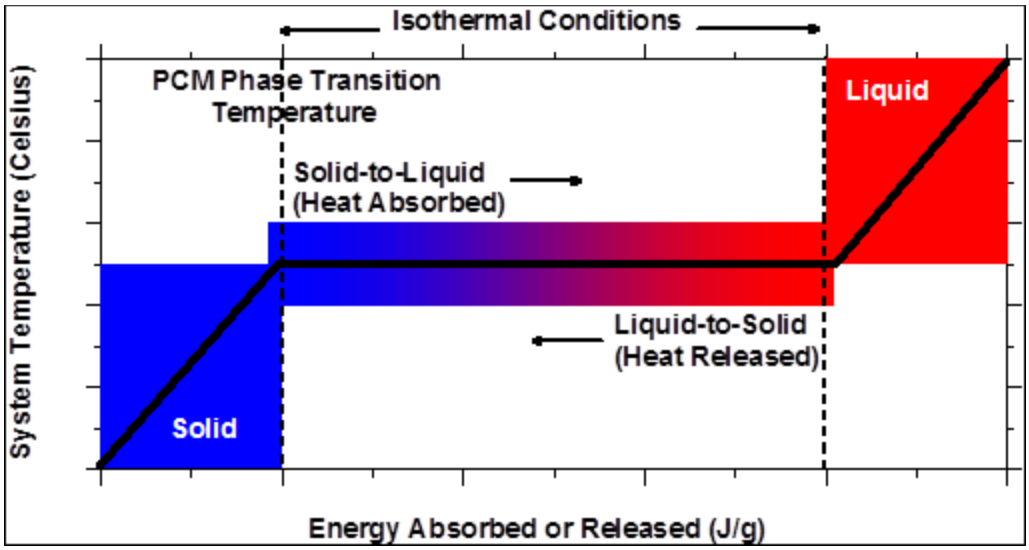

Figure 0-1: latent heat and sensible heat storage [18] , latent heat storage indicated by the horizontal line at isothermal conditions, while sensible heat storage is indicated by the sloped lines before and after the change of phase

There have been many studies focusing on shifting heating and cooling loads from a peak electricity period to an off peak period via the use of PCM [10]. This is done, for example, in a warm climate where a PCM with solid to liquid phase change is used to absorb heat from the building thus decreasing the load on air conditioning systems during the day, and returning to a solid when the temperature cools at night releasing heat into the environment. This strategy shifts the power consumption requirements for cooling in a warm climate to the evening and night time, rather than during peak high temperature times during the day [12]. This would allow power companies to reduce power generation during peak times as power requirements become more uniform throughout the day, enabling a reduction in emissions, during peak times which would also help reduce the cost of electricity by leveling demand [12].

2.1.1 PCM Classification

There are three main classifications of solid-liquid PCM; organic compounds, inorganic compounds and inorganic eutectics. Figure 2-1 shows the classifications of PCM.

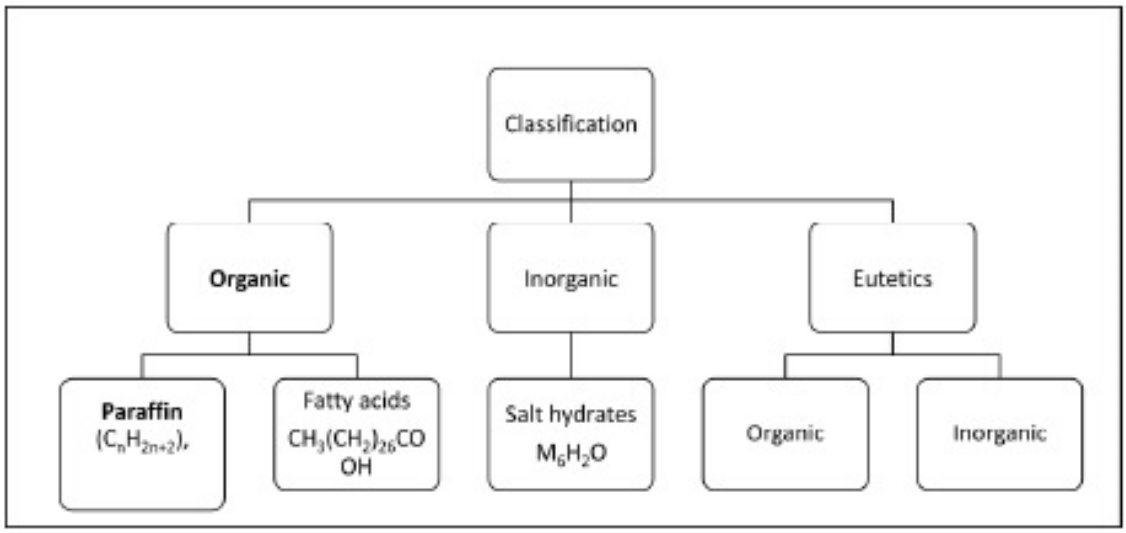

Figure 0-2: Classification of Phase Change Materials "reprinted from Pasupathy et al" [19]

Typically organic PCMs have two subgroups; paraffin and non-paraffin. Paraffins are waxes, which are affordable and supply a thermal storage density of approximately 120 kJ/kg up to 210 kJ/kg [3]. They are composed of hydrocarbon chains of $CH_3(CH_2)_nCH_3$. Paraffins have the advantages of being chemically inert, tend to have low vapor pressure during melting, they melt congruently, and can withstand thermal cycling. These materials work well in concrete applications because they are inactive in alkaline medium (unlike many other PCMs) and are resistant to degradation in the high pH environments associated with concrete [20]. Paraffins are non-polar substances such that hydrogen bonding with concrete hydrates is not possible [20]. Being linear alkanes, their methylene segments are capable of crystallization induced by high symmetry and weak van der Waals interactions [21]. The primary disadvantage of paraffins include a low thermal

conductivity of around 0.2 W/(mK) and a more significant change in volume during phase transition [3]. This low thermal conductivity can reduce the effective efficiency of the PCM due to super cooling or nonlinear melting.

Non-paraffin PCMs include organic materials such as fatty acids, esters, alcohols and glycols. While they have excellent melting and freezing properties, adapted for thermal storage, they have a significantly higher cost (about three times the cost of organic paraffins) [3, 14].

Inorganic PCMs have higher heat of fusion than most organic PCMs, good thermal conductivity, affordable and are non-flammable [3]. Hydrated salts are typical inorganic PCM used, and have a high storage density (about 240 kJ/kg) and a higher thermal conductivity than paraffin waxes, 0.5 W/(mK) [3]. Glauber's salt ($Na_2SO_4H_2O$) is a salt hydrate with a meting temperature range from 32 to 35 ^{0}C, latent heat of 254 kJ/kg, and it is one of the least expensive materials which can be utilized for thermal energy storage, but however the use of this material is restricted due to super cooling and phase segregation, which causes inefficiency in the thermal storage capabilities of the PCM [22]. A major drawback to hydrated salts is that they do not do well with thermal cycling; it melts congruently with formation of lower salts resulting in an irreversible process, thus resulting in a decreased storage capacity with each subsequent cycle [3].

Eutectics PCMs are a mixture of multiple solids that are proportioned in such a way to produce as low a melting point as possible. There are three groups of eutectics: organic-organic, inorganic-inorganic, and inorganic-organic.

2.2 PCM Incorporation into Building Materials

Phase change materials have been incorporated into a number of building materials including gypsum board [4, 5, 6, 7, 8, 9, 10, 11], masonry walls [12, 13]such as bricks or concrete, natural stone [23], asphalt and concrete [24, 25]. The techniques used to incorporate PCM into building materials include: (i) direct incorporation, (ii) immersion, and (iii) encapsulation [26]. Direct incorporation and immersion are methods for including PCM directly into the material during the manufacturing process. Immersion processes impregnate a porous construction material such as gypsum, brick or concrete blocks with PCM such that the pores adsorb the PCM in its liquid via capillarity forces [27]. Immersion and direct addition can have leakage issues allowing the PCM to flow out of the material system or incompatibility issues with the system itself such as alkaline sensitive PCMs degrading in high alkalinity environments. Encapsulation is another option for adding PCM to construction materials. This methodology entails the encapsulation of PCM in polymer shell usually done by the manufacture or into other materials that could then be incorporated into the building material. This methodology is proposed to reduce incompatibility issues along with leakage as the PCM is encapsulated and prevented from direct contact with the construction material [3]. Encapsulation of PCM occurs before incorporation into the building element, avoiding some of the issues associated with immersion and direct addition. Regin et al. stated the goals of PCM containment should be: (i) meet strength requirements and provide structural stability,(ii) be flexible, (iii) corrosion resistant and act as a barrier between the PCM and its environment, (iv) thermally stable, and (v) allow for good heat transfer [28]. One method of encapsulation is termed microencapsulation, which is a process where small particles

or droplets of the material are surrounded or coated with a thin film, a polymeric shell. This typically generates a capsule in the size range of micrometers to millimeters [28]. Microencapsulation prevents PCM leakage during phase change thus allowing PCM integration without interference with the building material, such as cement, lime, concrete, mortar, artificial marble, sealants, paints, textiles, and other coatings [15]. Macroencapsulation provides the same benefits of encapsulations such as leakage protection, while generating particles small enough for integration without interference with the building material. The use of macroencapsulation in construction is commonly done by either packaging the PCM into larger containers or, spheres, or casting them in panels that are then used directly as building elements. Shape-stabilized PCMs are another new material of interest, and is a combination of the PCM incorporation methods, typically using one material for microencapsulation (done via immersion or direct incorporation) before being placed into the main building element. These materials have a high specific heat, good thermal conductivity, as well as the ability to maintain shape during the phase change process [29]. This would enable their use in lieu of macroencapsulation and microencapsulation using polymeric shells. One example of the use of this type of PCM is used in a method for incorporation into wallboard as proposed by Min et al. discussed in the next paragraph.

Practical use of phase change materials requires first determining adequate locations for phase change materials to be used. One such possibility, is incorporation into wallboard, as gypsum wallboard is an extremely common building material used in almost all building projects, and several studies have been completed investigating incorporation of PCM into wallboard [8, 9, 11, 12]. One method for incorporation into wallboard was

proposed by Min et al. where melted paraffin was blended with perlite using two techniques: (i) at ambient temperature and atmospheric pressure in a 70^0C water bath, and (ii) using a vacuum adsorption method where the vacuum was drawn for 30 minutes followed by addition of the melted paraffin to the vacuum machine for another 30 minutes, both of which was then blended with water and gypsum and formed in molds [11].

Romero-Sanchez et. al. studied immersion of a natural stone, Bateig azul, into two different PCMs Micronal DS 5000X, and Rubitherm RT6 with the melting temperatures of 26^0C and 8^0C, respectively. Scanning electron microscopy (SEM), porosimetry, and differential scanning calorimetry (DSC) were the experimental techniques used for characterization of the natural stone with and without PCM. Large scale testing was completed by constructing small concrete buildings with a natural stone façade, treated and untreated with PCM. Measurements were recorded at various locations along the structure, every 10 minutes for several day-night cycles during the summer and winter [23]. They concluded that reduction in energy consumption would occur, but that the effectiveness is dependent on PCM melting temperature, construction location and treatment of a single piece of natural stone with PCMs with different melting temperatures would optimize energy savings in both winter and summer [23].

2.3 PCM Incorporation into Cementitious Systems

PCM can also be incorporated into cementitious systems such as concrete by a variety of means: (i) immersion of cured concrete into a melted liquid PCM, (ii) impregnation via saturation or vacuum saturation with porous aggregates [30], (iii) direct mixing of either encapsulated PCM or bulk PCM into concrete during mixing. The method selected for

incorporation will influence not only the thermal properties of the parent concrete, but also the mechanical strength [31] and durability performances [20, 24]. Concrete is a highly alkaline materials, and the pore solution of concrete maintains a significantly high pH environment [20]. Several PCMs have been shown to be unstable in alkaline medium and when exposed to a high pH environment. In addition, chemically some polar PCMs experience hydrogen bonding with silica hydrates in concrete and the hydroxyl ions from $Ca(OH)_2$, affecting their incorporation into the system [32]. There are also known issues with PCMs in concrete associated with the relation between PCM addition and the overall mechanical performance of the concrete [22, 25, 33]. The cause of this decrease in mechanical performance has been attributed to chemical and physical interactions between the PCM and the cement hydration products, perhaps resulting in the formation of alternative hydration products or decreasing the C-S-H formation as well as the microstructural influences or inclusion of a weaker phase into the binder of cementitious systems. Further, as the nature of phase change material is to absorb heat, it may result in a reduced curing temperature for the concrete as it absorbs heat that is being generated by the exothermic hydration reaction, perhaps resulting in a lower degree of hydration as compared to OPC mixes without PCM [24]. Additionally, it is notable that the temperature effects of PCM inclusion during the hydration processes may decrease the induced thermal stresses from the hydration reaction, possibly resulting in a final product that has increased overall mechanical and durability/transport performance due to decrease thermal cracking [24].

2.3.1 Incorporation into LWA

Lightweight aggregates in concrete usually serve to supply extra water that is used by the cement and pozzolan compounds during hydration as well as reducing overall structure weight. LWA materials are typically composed of porous materials. The porous nature of the LWA provides for the opportunity that they may be filled with PCMs using impregnation techniques such as vacuum saturation. Theoretically a LWA with 20% porosity can provide up to 350 kg/m^3 of PCM for a typical concrete system [3].

Bentz and Turpin ran DSC experiments on lightweight aggregate soaked in PEG and paraffin PCM. They were able to determine that the peak transition temperature for paraffin was higher than that of PEG and that heat transfer was enhanced between the PCM in the aggregate and the bulk concrete [24]. This can be attributed to affects in PCM in pore systems.

Bentz and Sakulich proposed the use of PCM incorporated into LWA in concrete for bridge decking, to reduce freeze/thaw damage. They developed a novel apparatus used to saturate low temperature PCM into the lightweight aggregate using several different PCMs to determine the optimal duration of vacuum saturation to impregnate into the LWA [30]. Compressive strength decreased for mortars with PCM present. Iso thermal calorimetry was utilized for analysis of hydration the samples using PEG saw retardation in hydration time and suppression in the peak of hydration. This showed that incorporation into LWA can still have negative effects on the mortars development.

Incorporation of the PCM butyl stearate into three different expanded clay and shale LWAs were studied by Zhang et al. to look at the pore structure of the aggregates along with the effective absorption of the PCM into the pores [34]. MIP and absorption testing

of the porous aggregate determined that for a pore space diameter of 1 to 2µm the PCM could occupy 75% of the total pore volume. This showed that vacuum saturation using expanded clay and shale as a good supporting material for PCM in concrete. DSC measurements illustrated that their method of vacuum saturating in concrete had comparable energy storage capacity to a commercially available PCM product [34].

2.3.2 Direct Incorporation

PCM stability in concrete was studied by Hawes et al. using autoclaved block, regular concrete block, pumice concrete, lightweight concrete using expanded shale aggregate, expanded slag aggregate, and ordinary portland cement (OPC). They immersed harden concrete specimens into liquid PCM. When selecting a PCM to be used in concrete many considerations need to be made concerning:

a) Thermodynamics: latent heat of fusion, heat transfer, transition temperature, phase equilibrium and vapor pressure;
b) Physical: appearance, change in volume and density;
c) Kinetics: avoiding supercooling, and the rate of crystallization;
d) Stability in the concrete;
e) Toxicity, flammability and nuisance;
f) Economy;

Out of these stability is considered to be one of the most important because if the PCM is unstable it will not preform perform well thermally [20]. Six different PCMs were selected; Butyl stearate, 1-dodecanol, polyethylene Glycol, 1-tetradecanol, paraffin and dimethyl sulfoxide. The thermal characteristics were done by differential scanning calorimetry (DSC) this was tested on samples aged up to 692 days to help determine the

stability. Some PCMs are instable in high alkalinity environments, such as butyl stearate, 1-dodcanol, and 1-tetradeconal, but using pozzolans like silica fume (SiO_2) and fly ash would reduce the alkalinity of the system and thus allowing for better stabilization of alkaline sensitive PCMs [20]. Butyl stearate was stable in the autoclaved block and regular concrete block, as well in the modified regular block, pumice concrete, and expanded shale. 1-dodecanol suffered some loss at initial stages in the autoclaved block then remained stable, while both dodecanol and tetradecanol had stable latennt heat in the modified regular concrete block and pumice concrete but experienced a phase change temperature shift downwards. Paraffin being alkane remained stable in the autoclaved block, regular block, pumice concrete and OPC, suffering little degradation with time and little leakage issues.

Typically direct mixing is done using a PCM that is encapsulated in a chemically and physically stable shell [35]. Encapsulation is to ensure no interference with the concrete, such as discussed in Hawes et al. Hunger et al. direct mixed Micronal, a microencapsulated paraffin into self-compacting concrete. Self-compacting concrete has a lower yield stress, simplifying concrete placement, and reducing the risk of fracturing the microcapsules [25]. It was found that the microencapsulated PCM had no influence on fresh concrete properties, though the peak temperature of hydration could be 28.1% reduced, thermal conductivity decreased, porosity increased and though there was a loss in compressive strength of 35 N/mm^2 was found to be acceptable for most constructional purposes.

.

Cabeza et al. ran a study on concrete blocks impregnated with Micronal, a microencapsulated PCM, used to build cubicles (2m x 2m x 3m) in Spain which were then tested for thermal efficiency. The results of the study showed that energy storage by encapsulated PCM led to an improved thermal inertia as well as a lower inner temperature, thus demonstrating the opportunity in energy savings [31]. The results also supported the importance of the night time cooling cycle that causes the PCM to freeze, allowing it to be used again during the day when it melts to complete a full cycle every day [31].

MATERIALS, MIXTURES AND METHODS

3.1 Materials

Materials utilized in this study are discussed and explained.

3.1.1 Cement

Type I/II ordinary portland cement (OPC) conforming to ASTM C 150 was utilized in preparation of mortars and cement pastes. Table 3-1 provides the chemical composition and physical characteristics of this cement.

Table 0-1: Typical chemical composition and physical properties of cement

Composition (% by mass) / property	**Cement**
Silica(SiO_2)	20.2
Alumina (Al_2O_3)	4.7
Iron oxide (Fe_2O_3)	3
Calcium oxide (CaO)	61.9
Magnesium oxide (MgO)	2.6
Sodium oxide (Na_2O)	0.19
Potassium oxide (K_2O)	0.82
Sulfur trioxide (SO_3)	3.9
Loss on ignition	1.9
Median Particle size (μm)	13
Density (kg/m^3)	3150

3.1.2 Pure Temp

Pure Temp is a proprietary formulized PCM that is produced by the company Entropy Solutions. It is made from 100% agricultural sources, making it biodegradable and non-

toxic. Pure Temp has a phase change transition temperature that varies from -40^{0}C to 150^{0}C allowing it to be used in many applications. It appears as a clear when in the liquid phase and appears as an opaque wax when in its solid phase. This bulk PCM shows consistent repeatable performance over numerous freeze/thaw cycles making it practical for applications in building materials. PT 25, 27, and 29, three of the Pure Temp PCMs, will be utilized in this research due to their phase change temperatures being, 25^{0}C, 27^{0}C, and 29^{0}C respectively, close to the human comfort level [3]. The bulk material will be used for direct incorporation into cement pastes, and impregnation into lightweight aggregates. Both PT 25 and PT 27 have a specific gravity of 0.85 while PT 29 has a specific gravity of 0.86.

Table 0-2: Material thermal properties of Pure Temp chosen for this research

PCM	PT 25	PT 27	PT 29
Onset (°C)	25.44	25.85	29.79
Peak (°C)	32.58	33.62	35.98
Enthalpy (J/g)	165.17	232.94	184.54

Onset and peak temperatures along with enthalpy values were determined using differential scanning calorimetry to be discussed in Section 3.3.1.

3.1.3 Lightweight Aggregate

The lightweight aggregate (LWA) used is provided by Stalite. The fine lightweight aggregate has a specific gravity of 1.80, and water absorption of ~ 9%. This aggregate is produced by heating pulverized pieces of slate in a kiln at around 2200 degrees Fahrenheit. High temperatures turn the slate molten allowing all the gases to evolve forming small unconnected voids. This aggregate will be used for the impregnation of Pure Temp PCMs for mortar mixes.

3.2 Mixture Proportions and Sample Preparation

Procedures for material preparation and mix proportions are discussed.

3.2.1 Saturation of LWA

Paraffin PCMs have very low thermal conductivity which can influence their ability to be an effective latent heat storage material; one way to improve this can be through impregnation into a more thermally efficient material such as LWA [24]. Furthermore, impregnation of PCM into LWA can potentially encapsulate the PCM reducing possible interference with the formation of hydration products.

Saturation of LWA by three different PCMs, PT 25, PT 27, PT 29 was implemented using three methods: (i) 24 hour atmospheric pressure saturation at 32^{o}C (to ensure that all the PCMS remain in a liquid state to facilitate penetration into the pores of the LWA), (ii) two hours of vacuum saturation followed by 24 hour atmospheric pressure saturation at 32^{o}C, and (iii) 24 hour atmospheric pressure saturation at 40^{o}C. Vacuum saturation was carried out using a vacuum desiccator set on a hot plate set to 60^{o}C to maintain the PCM in the liquid phase. Once saturation is completed, the LWA was placed in strainers and left to drain at 32^{0}C for two hours before being placed into an oven to dry for 24 hours. Two oven temperatures were utilized for the drying operation: 40^{o}C and 60^{o}C for methods (i) and (ii), while for method (iii) a drying temperature of 75^{o}C was employed.

Specific gravity of this saturated LWA was found using the following equation:

$$SG_{\text{saturated sand}} = \frac{100}{\frac{\%PCM}{SG_{PCM}} + \frac{\%LWA}{SG_{LWA}}} \quad (1)$$

Where SG_{PCM} and SG_{LWA} are the specific gravity for the PCM and LWA, respectively. The % PCM is the amount of PCM absorbed percentage into the LWA as obtained using the enthalpy of the LWA-PCM composite determined using DSC (Section 5.1.1). Specific gravity for the PCM was provided by the manufacturer, and the specific gravity and absorption of LWA was determined using the Arizona Department of Transportation (ADOT) ARIZ 211c (modification of AASHTO T84) method.

The ARIZ 211c is used for the specific gravity and absorption of fine aggregate executed by the following steps: 1) 1200 gram represented sample is dried at 110 +/- 5^{o}C to constant mass, 2) cover with water and permit to stand for 15 to 19 hours, 3) decant excess water and dry on a non-absorbent pad exposing the surfaces to a gently moving current of warm air, mixing frequently, 3) test sample by placing cone smoothly on the non-absorbent surface then proceed to add sand loosely in the mold until it is overflowing from the top and then lightly tamp for 25 times, if one side of the fine aggregate slumps when the mold is removed it is considered surface dry, 4) measure and record mass a pycnometer filled to its calibration capacity, 5) partially fill with water and introduce 500+/- g of saturated surface-dry fine aggregate, 6) fill with 90% the total capacity, roll and invert pycnometer to release all air bubbles, then fill to 100% capacity, 7) measure mass of the filled pycnometer, 8) empty out fine aggregate and dry to constant mass at a temperature of 110 +/- 5^{o}C, measure mass of dried sample. Finally calculations for bulk oven dried, bulk surface saturated dry, and apparent specific gravity can be done along with the percent absorption.

3.2.2 Coating of LWA

A cement paste having a water-to-cement ratio (w/c) of 0.75 was used to coat the PCM saturated sand, which would allow for complete encapsulation. It was placed in a strainer which was then vibrated to ensure LWA grains remained separate while being coated. The resulting aggregate was then spread over parchment paper, and was allowed to dry in ambient conditions covered for 72 hours before being stored. The specific gravity of the LWA with cement paste coating was determined using the specific gravities of the LWA + paste and PCM based on percentage as follows utilizing the combined specific gravity:

$$SG_{\text{coated sand}} = \frac{100}{\frac{\%PCM}{SGPCM} + \frac{\%(LWA+paste)}{SG(LWA+paste)}} \quad (2)$$

Where SG_{PCM} and $SG_{LWA+Paste}$ are the specific gravity for the PCM and LWA+paste, respectively. % PCM was found through enthalpy results using DSC. SG(LWA+paste) of was determined by the same method presented above (ARIZ 211c).

This coated saturated sand specific gravity was used for the mix designs for the mortars.

3.2.3 Mortar Mixes

Specific gravities (SG) that were used for mix proportions were based on MSDS documents (PCM), ARIZ 211c (LWA & LWA+ paste) and Eq. 1 (saturated sand) and 2 (coated saturated sand) as shown in Table 3-4.

Table 0-3: Specific gravity of materials used in mortar mixes

Specific Gravity	
Cement	3.15
Water	1
LWA	1.65
Saturated LWA (PT 25)	1.44
Saturated LWA (PT 29)	1.5
Coated LWA (PT 25)	1.5
Coated LWA (PT 29)	1.55
PT 25	0.86
PT 29	0.85

Mortars were prepared using a commercially available Type I/II OPC, water, LWA, and PCM. Mixture proportions were completed such that the cement volume was held constant; the sand volume fraction was 50% and a constant of w/c 0.4 by mass. The amount of PCM was set to be that in the coated sand volume. This mixture proportioning resulted in a PT 25 and PT 29 volume fraction of 5.97% and 3.94% respectively. A reduction in volume fraction of saturated LWA would be done utilizing thermal enthalpy results in order to keep the mix proportioning for PCM volume constant by using plain LWA as a percentage of the total sand volume. A summary of the mix design used in this study is presented in Table 3-5.

Table 0-4: mix proportions by volume in mL for 100 g samples size

Mixture	OPC (w/c 0.4)	PT 25 Sat Sand	PT 25 Coated Sand	PT 25 (5.97%)	PT 29 Sat Sand	PT 29 Coated Sand	PT 29 (3.94%)
Cement	22.68	22.68	22.68	22.68	22.68	22.68	22.68
Water	28.57	28.57	28.57	28.57	28.57	28.57	28.57
LWA	51.25	32.35	----	48.19	31.55	----	49.23
Saturated LWA (PT 25)	----	18.89	----	----	----	----	----
Saturated LWA (PT 29)	----	----	----	----	19.69	----	----
Coated LWA (PT 25)	----	----	51.25	----	----	----	----
Coated LWA (PT 29)	----	----	----	----	----	51.25	----
PT 25	----	----	----	3.06	----	----	----
PT 29	----	----	----	----	----	----	2.02

3.2.4 Cement Paste Mixes

Specific gravities used in mixture proportioning for cement paste mixes were used as provided by the MSDS.

Table 0-5: Specific gravity for materials used in cement paste mixes

Specific Gravity	
Cement	3.15
Water	1
PT 25	0.86
PT 29	0.85

Cement pastes were prepared with commercial Type I/II OPC, water and liquid PCM. Cement volume was held constant along with water content, such that the PCM was added as an additional volume to the mix. Table 3-7 presents the mix proportions by volume.

Table 0-6: mix proportions by volume in mL for 100 g samples size

	w/c 0.3	w/c 0.3: 10% PT 25	w/c 0.3: 30% PT 25	w/c 0.3: 30% PT 29	w/c 0.5	w/c 0.7	w/c 0.7: 10% PT 25
Cement	24.42	24.42	24.42	24.42	21.16	18.67	18.67
Water	23.08	23.08	23.08	23.08	33.33	41.18	41.18
PT 25	----	4.75	14.25	----	----	----	5.99
PT 29	----	----	----	14.25	----	----	----

3.2.5 Synthetic Pore Solution

The synthetic pore solution made was prepared using the methodology as proposed by Mammoliti and as modified from Berke and Hicks [36]. The synthetic pore solution consists of 0.6 M KOH, 0.3 M NaOH, and 12.50 g of solid $Ca(OH)_2$ per liter of solution [37].

PT 25 was added in 10% and 30% by volume additionally to determine if there are any chemical, thermal or bonding changes occurring in the pore solution in presence of PCMs.

3.3 Test Methods

Testing methods used are discussed with a brief background on the method.

3.3.1 Differential Scanning Calorimetry

A Perkin Elmer DSC 6000 was used to carry out DSC studies on pure PCM, pastes, saturated LWA and coated LWA to determine the onset and peak temperatures (^{0}C) and the enthalpy of the material (J/g) during phase change. This is a thermo-analytical technique that measures the heat released (exothermic) or heat absorbed (endothermic) during temperature scans. DSC is commonly used to determine material characteristics

such as glass transition temperature, phase change temperatures, and heat of fusion [21]. Sample sizes ranged from 13.0 mg to 30 mg. The thermal method used included a temperature sweep heating the sample from -20°C to 60°C followed by a ramp down cooling the sample from 60°C to -20°C in a pure nitrogen environment at a rate of 5°C/min. One complete heating/cooling cycle was completed for all samples twice. The equipment used is very sensitive and can detect heat flows in the range of ± 175 mW with an accuracy of ± 2.0% and precission of 0.1%. However, DSC measurements do have some draw-backs, such as a small sampling size that may not reflect the bulk material. PT 25, PT 27, and PT 29 scans with the peak temperature and enthalpies labeled are shown Figure 3-1.

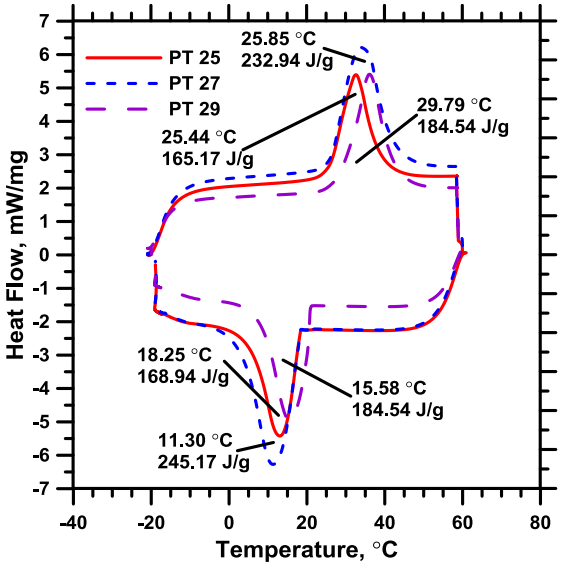

Figure 0-1: DSC heating and cooling scans for PT 25, 27, & 29

The above figures demonstrate the heat flow experienced by the samples for a single heating/cooling cycle. The peaks seen are where phase change is occurring, with the onset temperature labeled above. The enthalpy was calculated using the area under the peak portion of the curve. The heating portion shows results of the onset range for each

material that conforms to the manufacture specifications. During the cooling scan it is clear that there is a temperature shift as the phase changes from liquid to solid. Lower surface temperatures would cause for a decreased time in completion of solidification. Thermal conductivity plays an important role in the solidification process and materials with lower thermal conductivity will delay the solidification process [38, 39].

3.3.2 Isothermal Calorimetry

Isothermal calorimetry is used to study the heat release of an exothermic reaction, such as cement hydration, overtime. The heat release signature can be indicative of changes in the reaction kinetics as well as degree of hydration due to variation in the mix design. These studies were performed on mortars and pastes over a 24 hour period at a temperature of 32^{o}C to ensure the PCM would remain a liquid. Duplicate samples weighing approximately 200 g were tested for the mortars an 100 g for pastes were tested.

All mix materials were stored in an oven set to 38^{o}C 24 hours in advance to mixing. Mixing was also conducted in this oven with the samples being loaded no later than 5 minutes after the addition of water. This method of oven storage and mixing was utilized to negate the loss of the dissolution peak that occurred during the time when samples mixed in ambient lab conditions (~25^{o}C) were being heated to 32^{o}C in the calorimetry.

3.3.3 Thermal Conductivity

Thermal conductivity experiments were run on the mortar mixes to find the thermal coefficient, using the test apparatus as pictured in Figure 3-2.

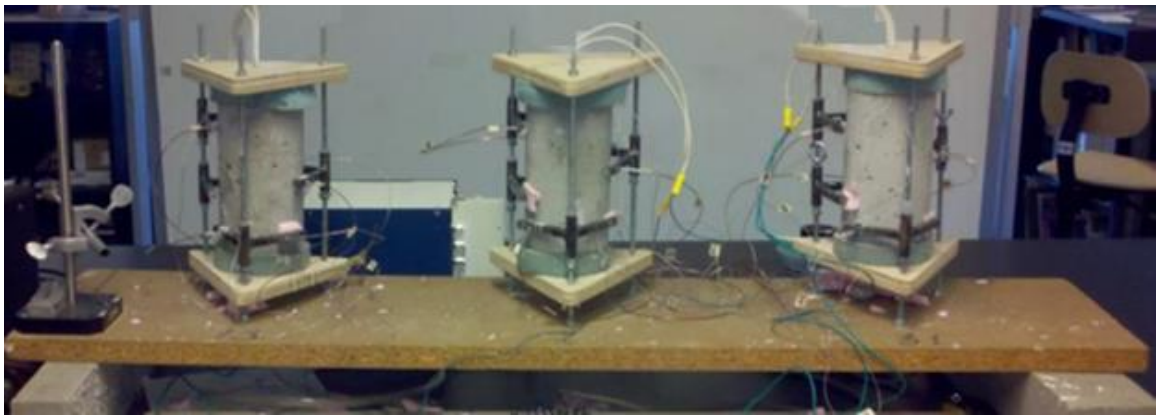

Figure 0-2: Thermal conductivity apparatus

This cylindrical specimen apparatus was first developed in 2006 by the National Center of Excellence (NCE) at Arizona State University and was later modified in 2011 to test with a larger cartridge heater with a diameter of 1.91 cm to be used for testing 10.2 cm diameter by 17.8 cm height cylinder samples [40]. Data measurement was collected via a National Instruments Data Acquisition (DAQ) system, using a virtual instrument (VI) created via LabView to store the temperature readings from the thermocouples. The equation used to calculate thermal coefficient is as follows:

$$k = \frac{(VI)\ \ln(r2/r1)}{2\pi L\ (T_1 - T_2)} \quad (3)$$

Where: V is 19.95 volts from the cartridge heating source, and I is 0.72 A the current from the heating source, and T_1 is the temperature at the inner radius of the cylinder sample as produced by the heating cartridge. Where: r_2 and r_1 are the outer and inner radius of the cylindrical samples, respectively and T_2 is the surface temperature of the cylinder.

The test was conducted over six hours with data recorded every minute from the thermocouples. Results were plotted as the inner radius temperature (T_1) vs. normalized

thermal conductivity. Normalized conductivity was calculated using the current thermal conductivity (k) divided by initial conductivity (k_o).

Normal thermal conductivity of lightweight concrete is reported to range from 0.4 and 1.89 W/m/K [41]. This range is dependent on a variety of conditions, such as type of aggregate, moisture condition and temperature [41].

All samples were moist cured for 10 days before being cut and cored and then air dried for 4 days before being tested.

3.3.4 Compressive Strength Testing

Compressive strength testing was performed on mortar and paste cubes in accordance with ASTM C 109. Three cubes with dimension of 5.08 cm were moist cured (~95% RH) in a chamber for 24 hours before being de-molded. The cubes were then placed back in the chamber until the desired testing age. Mortar cubes were tested at 3, 14 and 28 days. Cement paste cubes were tested at 3 days and 28 days. This test was done with the intent of comparing the effects of PCM on the mechanical properties of the mortar and paste.

3.3.5 Fourier Transform Infrared Spectroscopy

Fourier transform infrared (FTIR) spectroscopy was performed on a Mattson Genesis FTIR fitted with a diamond-headed attenuated total reflectance probe. FTIR is a method of infrared (IR) spectroscopy, where IR radiation is passed through a sample and some of the IR radiation is absorbed and some is transmitted (passed through). The resulting spectrum represents the signature of the microstructure of the sample. This makes FTIR useful to analyze any bonding that may be occurring in cementitious systems due to

PCM. Three replicates for each sample were completed. Pure PCM, Stalite LWA and mortars at 3, 14 and 28 days samples were taken and their spectrums were analyzed. The synthetic pore solution was tested at 1, 1, 14 and 20 days.

The FTIR spectra for PT and Micronal are presented in Figure 3-4.

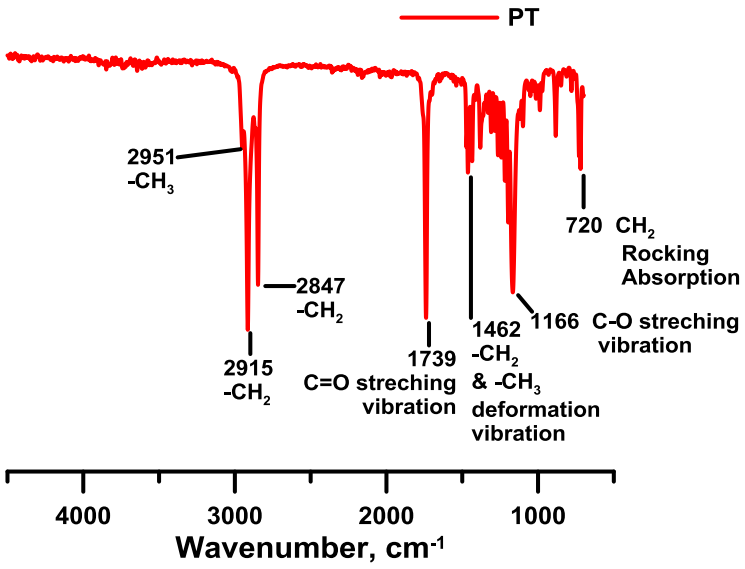

Figure 0-3: FTIR Spectrum for PT and Micronal

All peaks appear below 3000 cm^{-1}, meaning PT is a saturated hydrocarbon [42]. There are three peaks at the wave numbers of 2951 cm^{-1}, 2915 cm^{-1}, and 2847 cm^{-1} corresponding to the asymmetrical vibration of the $–CH_3$ functional group, $-CH_2$ functional group and the symmetrical vibration of the $–CH_2$ functional group, respectively. The wavenumber around 1730 cm^{-1} is the stretching vibration of the carbon double bonded with oxygen. The peaks in the range at 1462 cm^{-1} for PT correspond to the $–CH_2$ and $–CH_3$ deformation vibration. The single bond carbon – oxygen stretching vibration appear around the range of 1160 cm^{-1}. CH_2 rocking absorption band is at720 cm^{-1}. The $–CH_2$ peaks are much intense than the first peak representing $–CH_3$, signifying

that there are more $–CH_2$ molecules than $–CH_3$. The FTIR spectrum for PT reveals that it has the same bonding present in paraffin.

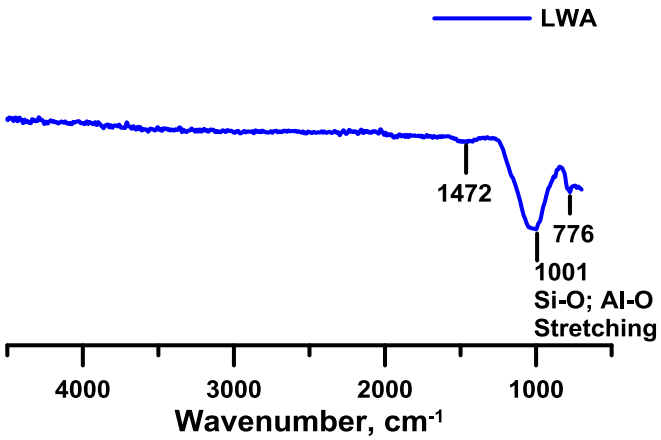

Figure 0-4: FTIR Spectra from Stalite LWA

The FTIR spectra for Stalite LWA indicated three distinctive peaks at 1472 cm^{-1}, 1001 cm^{-1} for Si-O and Al-O stretching, and 776 cm^{-1}.

3.3.6 Mercury Intrusion Porosimetry

Mercury intrusion porosimetry is a method used to determine information about the pore structure of a porous sample. Mercury is injected into a sample at a varying pressure, and the Washburn equations used to relate the intruded volume and pore diameter. MIP measurements were performed on hardened cement pastes at ages of 3 and 28 days using a Quantachrome PoreMaster instrument with a maximum intrusion pressure of 414 MPa. Duplicate samples of approximately 0.7 g were loaded in the 0.5 cc sample cells. MIP measurements have been shown to have several limitations, including the necessity of drying or otherwise preparing samples which may result in changes to the pore structure, possible inaccuracies in pore volume measurements due to the so-called “ink bottle” effect, wherein a large with a small entryway is considered a large volume of the smaller

diameter pore due to the high pressure required for mercury to enter the passage [43, 44, 45]. Further, in some samples, the high pressures present in MIP measurements may result in localized fracture and pore collapse [45].

3.3.7 Thermogravimetry Simultaneous Thermal Analysis

Thermogravimetric studies measure the weight loss associated with heating a sample over a defined range. In cementitious materials, the weight loss is primarily associated with the loss of free water from the pore solution, the dehydroxylation of both calcium hydroxide and C-S-H gel, as well as the decarbonation of carbonates present. TGA-STA measurements allow for the combined determination of both the weight loss and the heat flow as the sample is heated over the selected range. These heat flow measurements often result in specific peaks that are indicative of the reactions presented above. Based on these measurements, TGA-STA can be used to determine the degree of hydration of a sample based on the amount of various hydration products that have formed. TGA-STA experiments were completed using a Perkin Elmer STA 6000 with samples taken from the core of cement paste samples cured for 3 and 28 days under sealed conditions at ambient temperature. A thermal procedure consisting of heating the sample at a rate of 15°C/min over a temperature range from approximately 50°C to 1000°C was utilized.

INFLUENCE OF PCM ON MECHANICAL AND THERMAL PROPERTIES OF CEMENT PASTE

4.1 Introduction

The goal of this chapter is to gain a better understanding of the mechanical and thermal changes occurring when PCM is directly added to cement paste. Testing on mechanical effects was executed: (i) MIP analysis was completed to understand how the micro-structure of the paste is changing, and (ii) compressive strength testing to understand the strength decrease. Isothermal calorimetry was completed looking at the heat evolution during hydration, and TGA-STA was completed to find the amounts of hydration product, and PCM in the system at varying ages. DSC was a tool used for the thermal efficiency of the material. Finally FTIR analysis on PCM interaction with synthetic pore solution was done to better understand the interaction between the two.

4.2 Mixing Process

Cement pastes with w/c 0.3, w/c 0.7 and 0.5 were used in the mix design in order to understand the affects between PCM in cement pastes with varying w/c, thus varying pore sizes, and conditions of the pore solution.

All mixes were done using ordinary portland cement (OPC) and bulk non-encapsulated PCM, in order to better understand the effects of direct PCM incorporation in cementitious systems.

During mixing some things became apparent that would affect the ability to use certain mix designs. A mix with a w/c 0.7 and 30% PT 25 by volume was attempted, but the PT 25 and the water would not mix with the cement. Once cement particles are coated with PT it becomes hydrophobic and will repel water, conversely when cement particles are

coated in water it repels PT 25. The water and PCM quantities were high enough that there was excessive liquid in the system. The result of this was a non-homogeneous mix, that when cured results in a low w/c past and a separated liquid of water and PCM. This mix was then discarded from further study. Optimal PCM introduction with w/c is very important because the liquid to powder ratio cannot be to high.

4.3 Compressive Strength Results

Compression testing was done on 7 different cement pastes. All mixes with PT 25 or PT 29 showed a decrease in strength at seven days but increased in strength by 28 days.

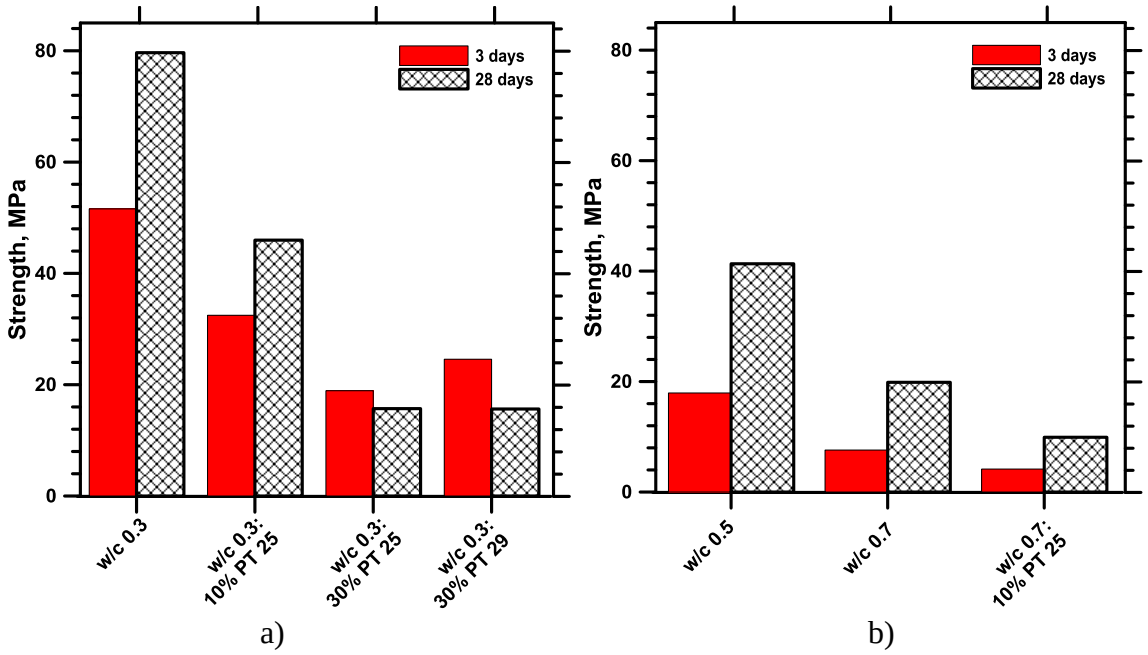

Figure 0-1: Compression strengths for a) w/c 0.3 mixes; b) w/c 0.5 and w/c 0.7 mixes

Mixes with 30% PT 25 or PT 29 had a larger strength decrease, over 50%, in comparison to the control at three days. All OPC mixes with 30% PT had a drastic decrease at 28 days, w/c 0.3 with 30% PT 25 at a 63% decrease at 3days, but an overall 80% decrease seen at 28 days, and w/c 0.3 with 30% PT 29 decreasing 52% at 3 days to 80% at 28

days. This shows that the PCM at 30% dosage in plain OPC mixes affects the long term strength development as well as early strength.

The decrease in strength can be attributed to the following: (i) the PCM's reaction with hydration products, (ii) reduction in the heat of hydration which contribute to earlier strength development [46] and (iii) changes to the pore structure.

It is a well-known fact that PCM does interact with C-S-H formation thus reducing strength [20, 24, 33]. This is due to the long chains of PT wraps around cement particles that cannot react to water [47] in addition to these cement particles unable to react they cannot be used as a nucleation point.

PCM also reduces the peak hydration temperature of the cement due to its thermal storage capabilities, this can be used to control thermal stresses and cracking which would help for long term strengths, but reducing the peak hydration will affect the early age strength [24]. The effects of PCM on hydration temperature and time will be further discussed in Section 4.5 using isothermal calorimetry.

Pore structure plays a factor in the mechanical strength of a cement paste. An OPC mix with a higher w/c will have greater pore volume and a larger critical pore diameter and lower compressive strengths. The addition of liquid PCM plays two main roles in effecting pore structure: (i) the addition of more liquid in the form of PCM into the mix increases the volume, and (ii) the reduced hydration keeps pores large and free of hydration products. MIP testing was executed in order to better understand the changes in pore structure; further discussion will be done in Section 4.4.

4.4 MIP Results

MIP testing was done on samples of all pastes at ages of 3 and 28 days to determine the pore volume of the paste. The MIP results for both intruded volume and critical pore diameter are in Figure 4-2 for the cement pastes after 3 days of curing.

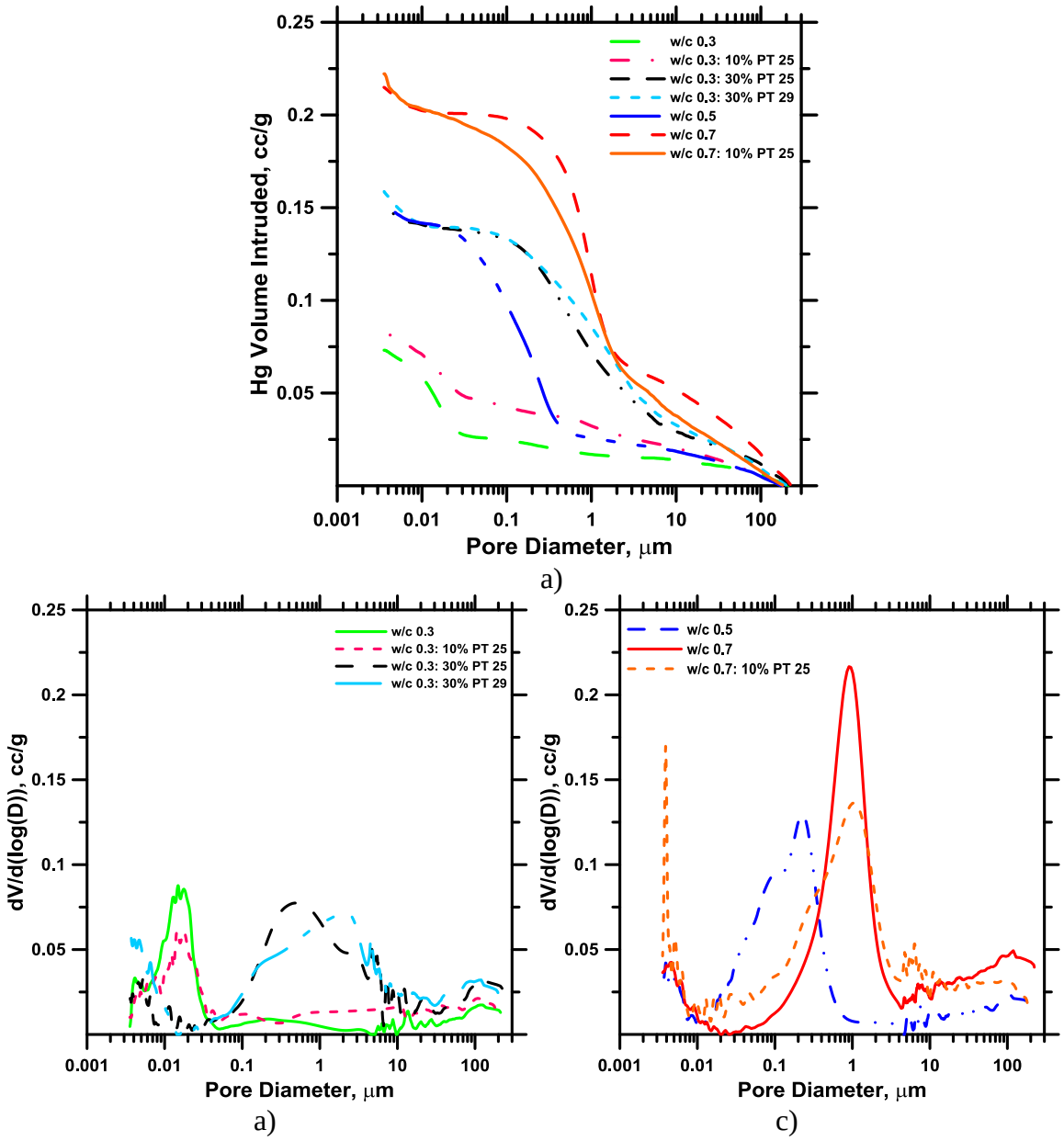

a)

a) c)

Figure 0-2: 3 day OPC mixes; a) mercury intrusion volume; b) pore size distribution for w/c 0.3; c) pore size distribution for w/c 0.5 and w/c 0.7

The volume intrusion as seen in Figure 4-2 a) ranged from, 0.07 cc/g for w/c 0.3 to 0.225 cc/g for w/c 0.7 with 10% PT 25. Figures 4-2 b) & c) illustrate the pore size distribution of the various mixes tested in this project, with the critical pore diameter indicated by the first major peak on these plots when looking from the smallest to largest pore sizes [48]. The critical pore diameter in considered to be an indicator of pore structure. Table 4-1 shows all the results for the intruded volume and critical pore sizes for each mix.

Table 0-1: Cumulative volume and critical pore sizes for pastes at 3 days

3 days	w/c 0.3	w/c 0.3: 10% PT 25	w/c 0.3: 30% PT 25	w/c 0.3: 30% PT 29	w/c 0.5	w/c 0.7	w/c 0.7: 10% PT 25
Cummulative Volume (cc/g)	0.07	0.08	0.15	0.17	0.15	0.218	0.225
Critical Pore Size (µm)	0.015	0.018	0.3	2	0.2	0.9	1

The lower w/c contents such as w/c 0.3 and w/c 0.5 both were shown to have a smaller intruded volume and critical pore diameter to the higher w/c 0.7 mix as predicted [49]. Mixes with the additional PCM volume were seen to have a larger intruded pore volume and pore threshold size than the corresponding control mixes. Mixes with 10% PT 25 showed similar pore size threshold as the control. W/c 0.3 and w/c 0.3 with 10% PT 25 showed a difference of critical pore diameter of 0.003 µm. W/c 0.7 and w/c 0.7 with 10% PT 25 had a pore diameter size increase of 0.1 µm. Both w/c 0.3 mixes with 30% PT an increase in the critical pore size diameters of 0.285 µm for PT 25 and 1.985 µm for PT 29, this is most likely due to the PCM causing a structural rearrangement of the packing density [25]. The mixes with PCM showed higher intruded volumes and pore distribution

because cement particles coated in PT could be used for cement hydration and could not be used as a surface for nucleation. This causes for less hydration products to form thus unable to fill the pore spaces. In addition the PCM was introduced into the mix as a liquid and thus increased the cement powder to liquid ratio.

At 28 days all PT mixes had higher intruded volumes than the control except for w/c 0.7 with 10% PT 25 mix. Volume intruded was substantial lowered based on more hydration products forming and thus pore sizes decreasing [49]. The range of intruded volume at 28 days ranged from 0.065 cc/g for w/c 0.3 to 0.19 cc/g for w/c 0.7 as seen in Figure 4-4 a).

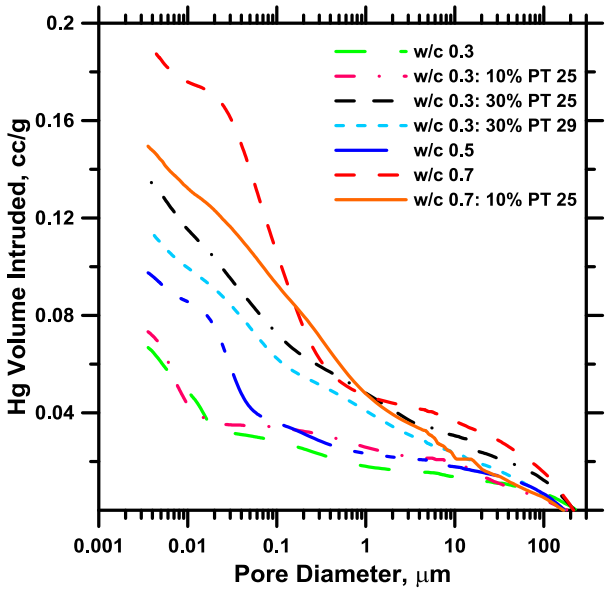

a)

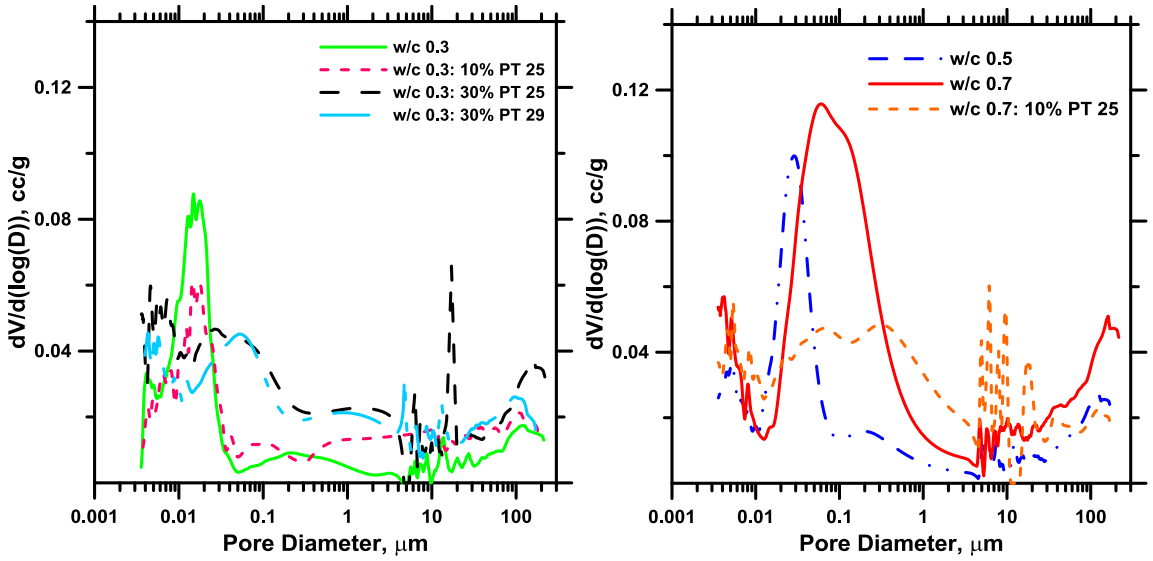

b) c)

Figure 0-3: 28 day OPC mixes; a) mercury intrusion volume; b) pore size distribution for w/c 0.3; c) pore size distribution for w/c 0.5 and w/c 0.7

Table 0-2: Cumulative volume and critical pore sizes for pastes at 28 days

28 days	w/c 0.3	w/c 0.3: 10% PT 25	w/c 0.3: 30% PT 25	w/c 0.3: 30% PT 29	w/c 0.5	w/c 0.7	w/c 0.7: 10% PT 25
Cummulative Volume (cc/g)	0.065	0.07	0.135	0.115	0.1	0.19	0.15
Critical Pore Size (μm)	0.013	0.017	0.04	0.04	0.02	0.06	0.1

The critical pore diameters for w/c 0.3 and w/c 0.3 with 10% PT 25 are 0.013 μm and 0.017 μm, respectively. A change in pore size distribution with curing age for w/c 0.3 was -0.002μm while the mix with 10% PT 25 was -0.001μm. There was a drastic shift in the critical pore size for w/c 0.7 from 0.9 μm at 3 days to 0.06 μm at 28 days, similar shifts in seen for both w/c 0.3 mixes with 30% PT, w/c 0.5, and w/c 0.7 with 10% PT 25, this is attributed to the curing time allowing hydration products to grow in the pore space [49]. This makes sense because mixes with a lower w/c have smaller pore size at early

ages, and less water to be used for initiation of hydration, meaning that the hydration process takes less time to fill these pores enough to slow the rate of pore size decrease.

4.5 Isothermal Calorimetry Results

Five mixes were analyzed for isothermal conductivity: OPC w/c 0.3, OPC w/c 0.7, OPC w/c 0.3 with 10% PT 25, OPC w/c 0.3 with 30% PT 25, and w/c 0.7 with 10% PT 25. Isothermal calorimetry is used to monitor the heat evolution and determine an approximate degree of hydration due to the exothermic nature of the cement hydration reaction. C_3S and C_3A have a high exothermic heat release of approximately -137.6 kJ/mol and -248.3 kJ/mol while the formation of C-S-H has a relatively low heat release of (-20 kJ/mol) [30].

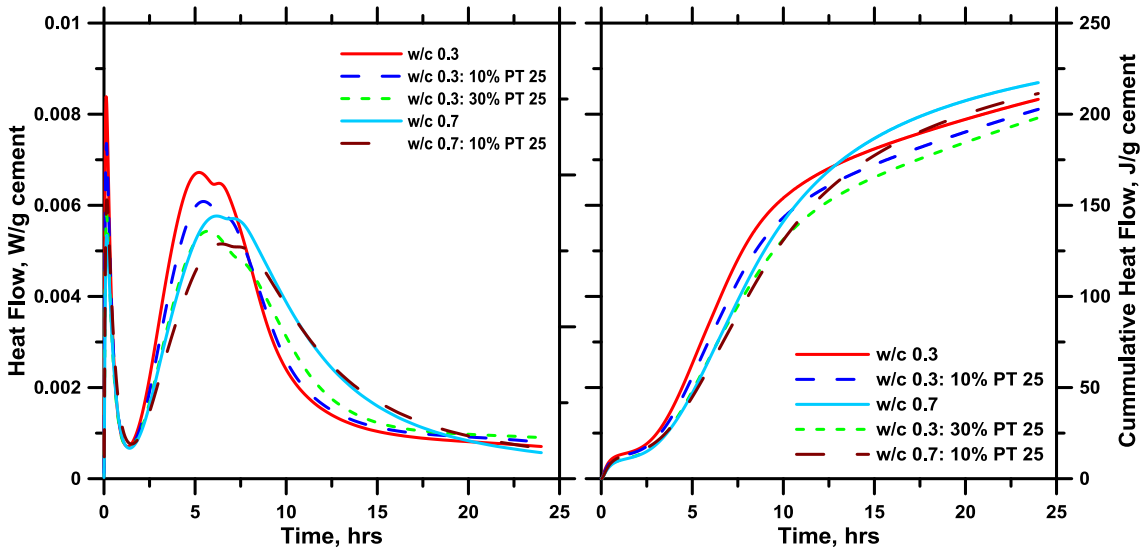

a) b)

Figure 0-4: Isothermal heat flow and cumulative heat flow for mixes noted.

The dissolution peaks as seen in the first few minutes is due to the rapid heat release that occurs when the cement minerals are dissolving and reacting with water to form the amorphous layer of hydration product around the particles, thus keeping the particles from further reacting. Mixes with PT had a lower heat flow during the dissolution period;

this is due to the long chains of PT wraps around cement particles that cannot react to water [47].

The acceleration period is when C_3S is hydrating and the rate of hydration is controlled by the rate of nucleation and growth of the hydration products.

In addition the maximum reaction heat flow is lower in mixes with PT 25, thus showing suppression of hydration. Between w/c 0.3 and w/c 0.7 there is a difference in reaction due to the dilution occurring to the excess mix water in w/c 0.7 OPC paste. As PT 25 is added into pastes it is seen that there is a clear depression in the heat flow, this depression gets greater as more PT 25 added as seen by the differences in w/c 0.3 with 10% PT 25 and 30% PT 25, this is partially due to the dilution affects similarly seen with a high w/c OPC.

Cumulative heat flow experienced at 24 hours indicates that the heat of hydration in the cement pastes with PT 25 is lower. The PT 25 is also delaying hydration as discussed above which will in turn affect early age strength development but can help with thermal stresses [24].

4.6 DSC Results

DSC analysis was performed on each paste mix at ages 3 and 28 days. All 3 day results had peak temperature occurring in the range of 29^0C to 30^0C for PT 25 and 31^0C to 32^0C for PT 29. These results are expected due to the adaption of the PT in the cement increasing phase change transition temperature.

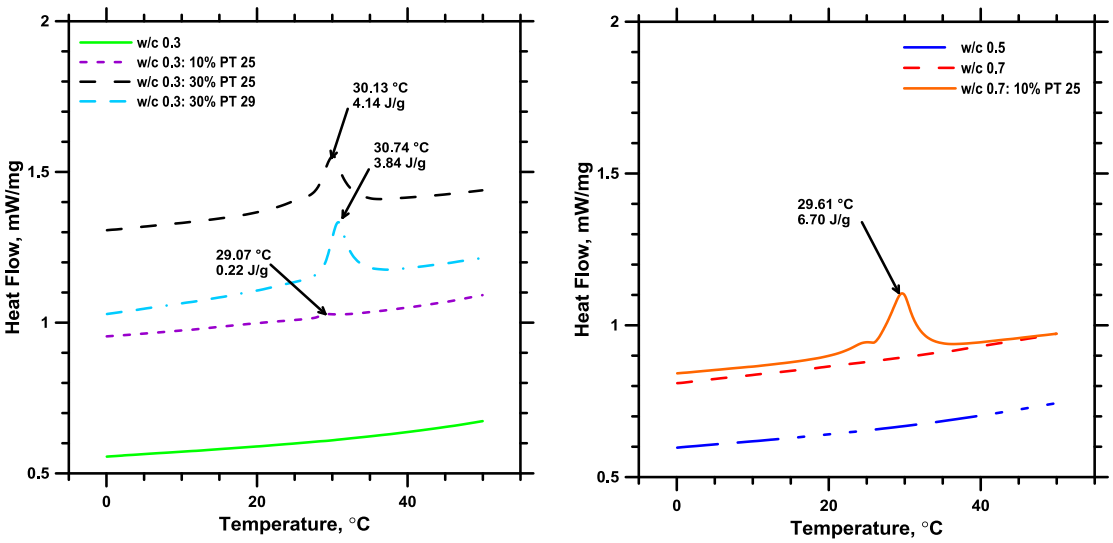

Figure 0-5: Heating and cooling scans at 3 days for a) w/c 0.3 mixes and b) w/c 0.5 and w/c 0.7 mixes

The phase change temperature was increased for PT 25 from 25.44^{0}C in bulk condition up to 30^{0}C in paste mix, while mix with PT 29 saw a smaller increase in the phase change temperature; this is due in part to the confinement in the pore structure. This is explained by Clapeyron equation (Equation 3) which will be further discussed in Section 5.1.1.

Table 0-3: Enthalpy and efficiency percentages for cement pastes at 3 days (efficiency of the mixes was calculated by the enthalpy of the mix over the theoretical enthalpy for the percentage by mass of PT in the mix. Name for each mix is in percentage of volume of PT added)

3 days	Pure PT 25	Pure PT 29	w/c 0.3: 10% PT 25	w/c 0.3: 30% PT 25	w/c 0.3: 30% PT 29	w/c 0.7: 10% PT 25
Enthalpy (J/g)	165.17	184.54	0.22	4.14	3.84	6.7
Efficiency (%)	----	----	3.40	23.00	21.53	82.87

The w/c 0.7 mix with 10% PT 25 by volume had the greatest efficiency, when compared to the w/c 0.3 mixes with PT. The higher efficiency can be attributed to the higher water content in the system is allowing for better thermal conductivity allowing nearly all the PT to phase change in the system.

Reduction in enthalpy continued with curing age as further illustrated by and DSC results at 28 days, which had a more significant enthalpy reduction.

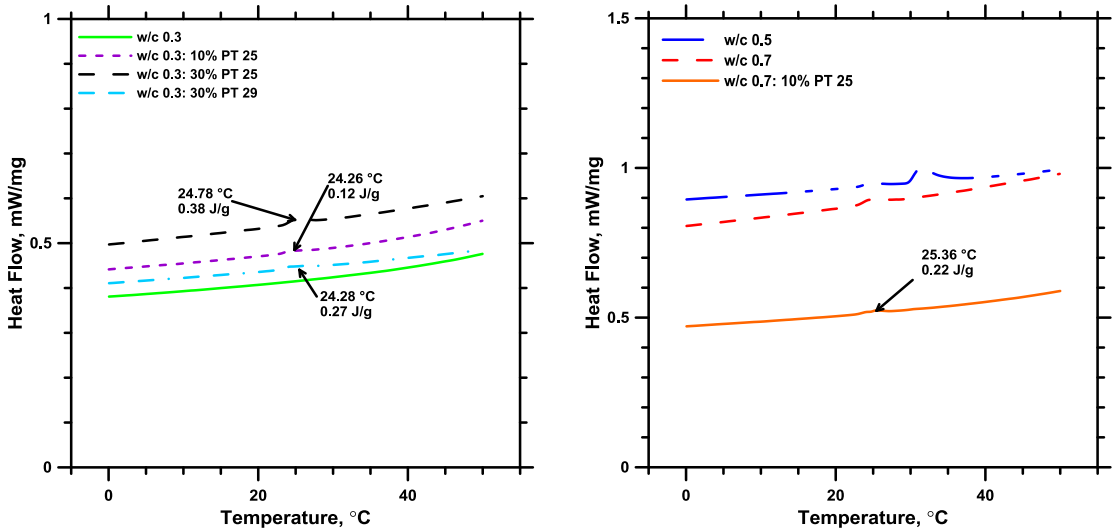

a) b)

Figure 0-6: Heating and cooling scans at 28 days for a) w/c 0.3 mixes and b) w/c 0.5 and w/c 0.7 mixes

The phase transition temperature for solid-liquid change shifts drastically between 3 and 28 days. At 3 days the phase change temperature is around 30^{0}C while at 28 days it is around 25^{0}C. This can be attributed to PCM confinement into a larger volume of smaller pores, because as the temperature begins to rise above the solidification point the PCM in smaller pores will begin to absorb latent heat at lower temperature than the PCM in the larger diameter pores [20]. The critical pore size decreases with curing age as seen in Section 4.4 this is one physical reason for reduction in enthalpy as seen at aging.

Efficiency results at 28 days were less than 3%, as seen below in Table 4-4. This is a drastic decline in efficiency which makes direct incorporation of PCM into paste not effective for increasing the thermal energy storage of concrete.

Table 0-4: Enthalpy and efficiency percentages for cement pastes at 28 days

28 days	Pure PT 25	Pure PT 29	w/c 0.3: 10% PT 25	w/c 0.3: 30% PT 25	w/c 0.3: 30% PT 29	w/c 0.7: 10% PT 25
Enthalpy (J/g)	165.17	184.54	0.12	0.38	0.27	0.22
Efficiency (%)	----	----	1.85	2.11	1.35	2.72

The percentage efficiency for the mixes was determined using enthalpy results from DSC scans, and taking the ratio of this result with percentage of mass of pure PCM that was added to the system. The mix incorporating 10% PT 25 into w/c 0.7 paste shows a greater efficiency than the lower w/c mixes, this can be attributed to the thermal conductivity of the water in the system aiding in the phase change capabilities of the PCM. There are several possible causes to this reduction including: the interaction with the pore structure [50], and the high thermal resistance attributed to the paste, which may hinder the heat transfer to the interior surfaces, thus causing melting to occur only near the heat sources.

Studies have shown that there can be an interaction between the PCM and the cement [24]. Paraffins are non-polar alkane where carbon and hydrogen atoms are linked via single bonds, making it chemically stable and less prone to hydrogen bonding. Paraffins are composed of linear chains where the end carbon atom has three hydrogen atoms while the interior carbon atoms have two hydrogen atoms as shown below, Figure 4.7.

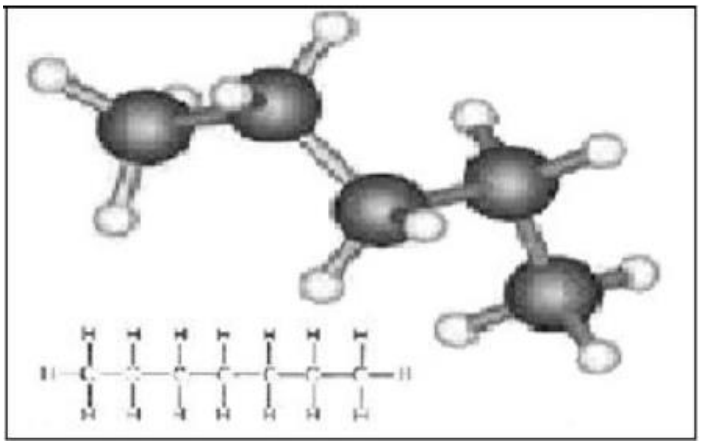

Figure 0-7: Chemical structure of Paraffin [2]

This reduction could be due to a random cross-linking of PT with CSH and other cement hydrates in the cement matrix similar to the study by Montserrat et al. of cross linking of Epoxy-diamine resins [51]. Enthalpy relaxation in epoxy-diamine resins was found to increase as the crosslinking lengths increased in the rate at which enthalpy relaxation occurred, additionally as annealing time increased more enthalpy relaxation would occur [51].

Enthalpy relaxation is thought to occur when there is a cooperative rearrangement of some of the molecular entities, specifically in the main-chain molecular segments in the case of linear polymers according to the Adam-Gibbs theory [52]. A study on enthalpy relaxation studies of polymethyl methacrylate networks with varying crosslinking degrees that the greater the cross linking density the higher the reduction in enthalpy [53].

A study performed by Dondi et al. analyzed silica crosslinking with polybutadiene and styrene-butadiene (SBR). Cross linking in this system occurs primarily through 3 stages; i) absorption of radiation energy in the silica particles followed by exciton migration at the surface, (ii) reaction at the surface of excited silica with absorbent SBR chains

leading to silica bonded free radicals, (iii) crosslinking of SBR initiated from grafted radicals [54]. Other methods can cause exciton migration and thus excitation in an atom such as: (i) thermal, (ii) chemical, (iii) pressure, or (iv) radiation.

This indicates that the significant reduction in enthalpy with these pastes is likely attributed primarily to cross linking of the PCM with the cement hydrates, primarily the silica in CSH. In addition there are physical interactions imposing depression effects on the latent heat storage conditions: (i) the latent heat of the confined PCM is experiencing non-freezing layers at the interface of the cement matrix [34], and (ii) an amount of confined PCM may not be taking part in the phase transition and thus would cause a depression in the latent heat [55].

The thermal efficiency with curing age is plotted below. It is clear from this plot that as the age increases there is a reduction in thermal efficiency.

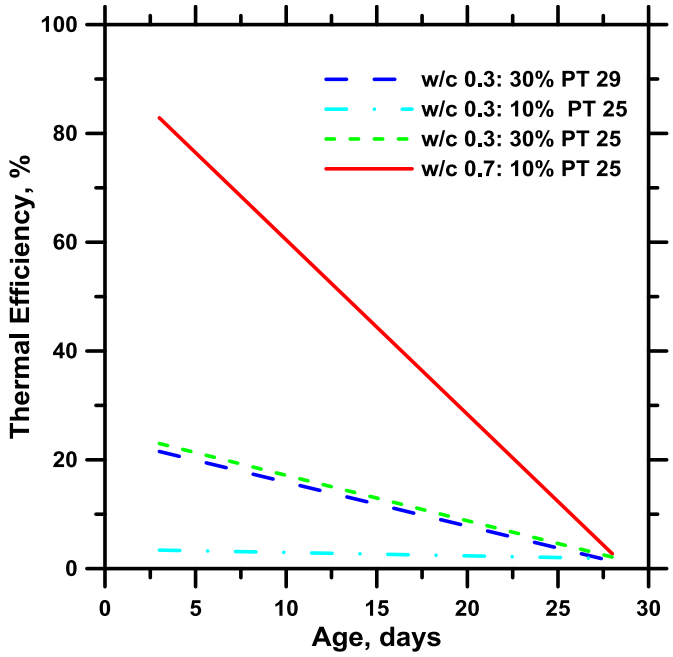

Figure 0-8: Thermal efficiency at varying curing ages

This can be attributed to a combination of things: (i) the crosslink density is increasing, (ii) as hydration progresses more pressure is placed upon the PT in the pores, and (iii) the thermal resistance of the paste is increasing with time as hydration products form.

4.7 TGA-STA Results

TGA-STA will be utilized for analysis of the thermal stability of the pure PT 25, pure $Ca(OH)_2$, a mix of $Ca(OH)_2$ with 30% PT 25 by volume at 11 days after mixing and cement pastes at 3 and 28 days of curing.

Figure 4-9 presents the thermal degradation of PT 25, $Ca(OH)_2$ and a mixture of $Ca(OH)_2$ with 30% PT 25 by volume at 11 days.

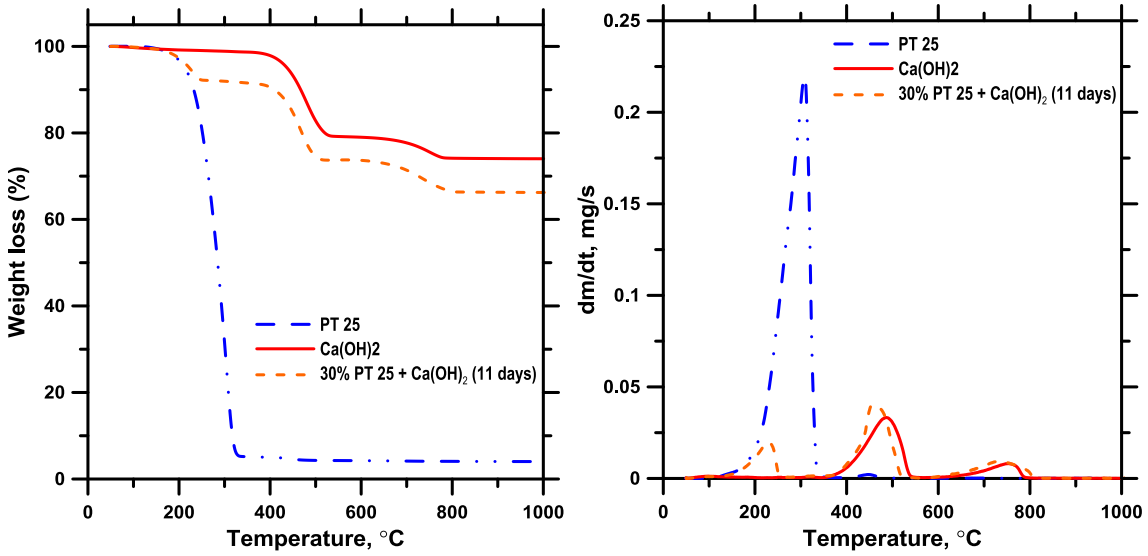

a) b)

Figure 0-9: 3 day TGA a) weight loss (%) & b) mass loss rate for pure PT 25, pure $Ca(OH)_2$, and 30% PT 25 + $Ca(OH)_2$ at 11 days.

95% of the weight of PT 25 was loss due to evaporations between 190°C and 320°C. This is where the PT is oxidizing [56]. By visual observation there was no sample left in the crucible after testing, just a thin residue at the bottom. Pure $Ca(OH)_2$ experiences higher

rate of mass loss between the range of 450°C to 550°C due to the dehydroxylation of $Ca(OH)_2$. There was a total weight loss of ~25% for pure $Ca(OH)_2$. The pure PT 25 and $Ca(OH)_2$ composite had a total mass loss of ~ 34%. Converting the percentage of PT 25 added by volume into mass of the complete sample the PT 25 is ~ 10% by mass. The mass loss difference between the pure $Ca(OH)_2$ and the sample with PT 25 and $Ca(OH)_2$ can be accounted as the evaporation of PT 25 from the system. There were two distinct changes in the mixed sample when compared to the pure samples: From the rate of mass loss plots it is clear that the temperature span that the oxidation of PT occurs is smaller from 190°C to 250°C and the rate of mass loss during the dehydroxylation period increased in the lower temperature range from 450°C to 490°C. This shows that the mass loss associated with PT in the system begins to extend into the mass loss associated with dehydroxylation of $Ca(OH)_2$. This makes the mass loss associated with PT and the mass loss associated with $Ca(OH)_2$ diffucult to distinguish from one another and thus hard to analyze for the amount of hydration products in the system via TGA-STA. In addition PT oxidizes in the same range as the evaporation of water in the system, making it difficult to separate those two events also.

There are three distinctive peaks in the dm/dt plots for pates at 3 days, around 100°C, 450°C, and 680°C, respectively. The mass loss seen before 300°C, is indicated by the first peak at 100°C. For OPC, this is attributed to the loss of free water within the pore structure of the paste as well as some water loss due to water bound to C-S-H. The mass loss between the range of 450°C to 550°C is the dehydroxylation of $Ca(OH)_2$ and the mass loss between the range 700°C to 900°C is the decarbonation of $CaCO_3$.

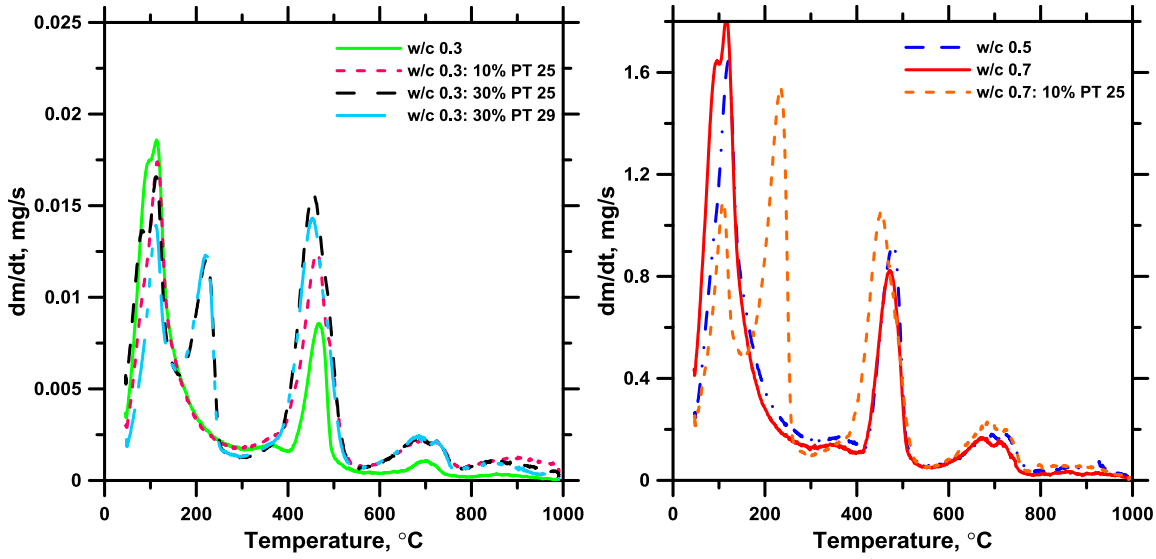

a) b)

Figure 0-10: 3 day TGA mass loss rate for OPC mixes

It is notable that with the mixes at 3 days curing with PCM have a fourth mass loss peak around 220°C is associated with the mass loss of PT as it is evaporating from the system from 190°C to 320°C.

Again there is an increase in the rate loss seen in the range for dehydroxylation of $Ca(OH)_2$ this is due to the PT in the system evaporating at a higher temperature due to cross linking with the $Ca(OH)_2$ in the pore solution. Further analysis of PT interaction with the pore solution will be discussed in Section 4.8.

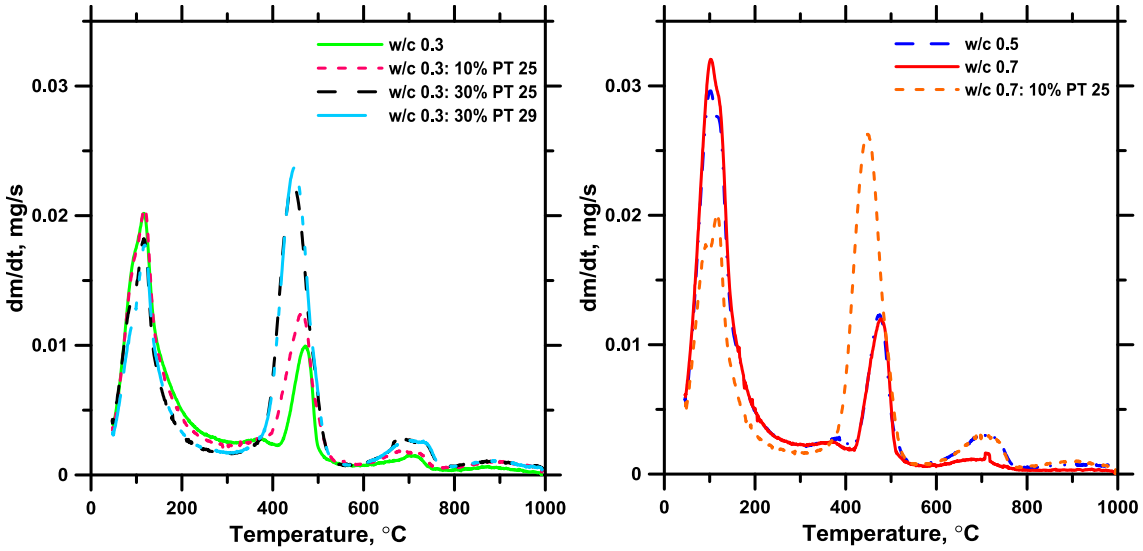

Figure 0-11: 28 day TGA weight loss % for OPC mixes

All PCM mixes show the similar trend of having a larger weight loss at the 450°C temperature range. At 28 days thermal analysis of the OPC samples shows a peak in the rate of mass loss around 220°C is not seen for any mixes with PT. This mass loss rate shifts toward 420°C. This is due to PT and CaOH crosslinking and the cross linking density increasing and thus improving the thermal durability of PT. Further analysis on hydration products percentages were not possible due to the cross linking of PT and $Ca(OH)_2$.

4.8 Synthetic Pore Solution

Synthetic pore solutions were prepared using and 10% and 30% of PT 25 was added to them by volume. These solutions were then mixed and specific quantities were stored in sealed vessels and kept in an incubator set at a temperature of 32°C. This temperature ensured that the PT 25 would remain in the liquid phase. The three samples were tested after storing in the incubator for 1, 5, 14 and 20 days.

Each time a sample was tested, it was shaken to ensure the sample was as homogenous as possible. For days 1 and 5 the PT 25 remained mostly a liquid with a very small amount

of particulate matter in the solution, the samples were able to be shaken and able to be taken as a representative sample. At 14 days the precipitate amount had grown making incorporation a bit more difficult, especially for the small sample sizes used for DSC and FTIR. By day 20 the PT 25 had precipitated to the point that shaking and mixing the sample was insufficient to reincorporate it into the solution. The semi-solid mass of PT 25 was white and gooey with the pore solution separated from the PT 25. Testing at 20 days for both DSC and FTIR using the representative mixed solution was impossible so the PT 25 semi-solid was analyzed with added pore solution.

4.8.1 FTIR

FTIR was performed on the synthetic pore solutions to track the bonds and their occurrence over time. This was done in order to see if a break down in the PT 25 bonds is occurring or if new bonds are forming between the synthetic pore solution and PT 25.

The $–CH_3$ functional group peak as seen for pure PT 25 cannot be detected in the synthetic pore solution spectrum. Another interesting effect noted is that the CH_2 rocking absorption peak is not detected until an age of 14 days.

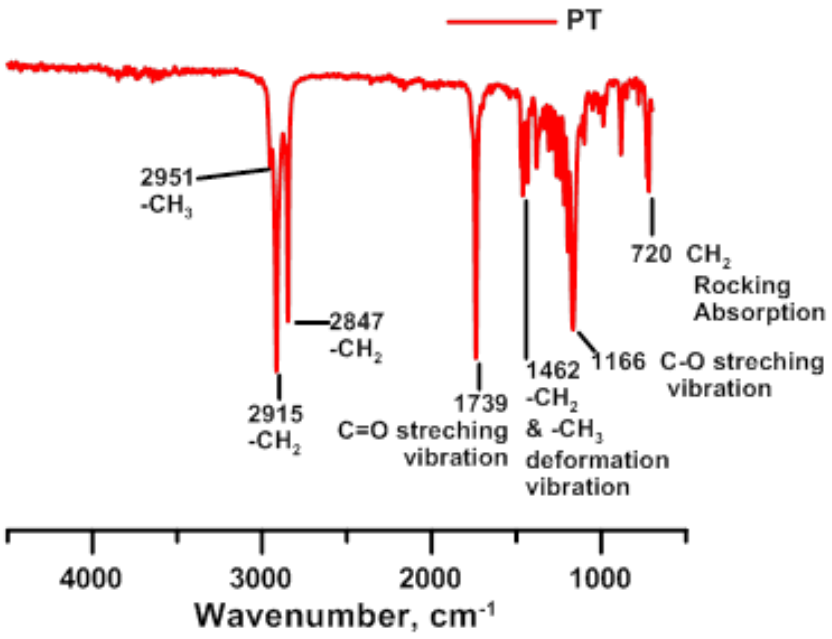
PT
2951
-CH3
2847
-CH2
2915
-CH2
1739
C=O streching
vibration
1462
-CH2
& -CH3
deformation
vibration
1166
720 CH2
Rocking
Absorption
C-O streching
vibration
4000
3000
2000
1000
Wavenumber, cm-1

a)

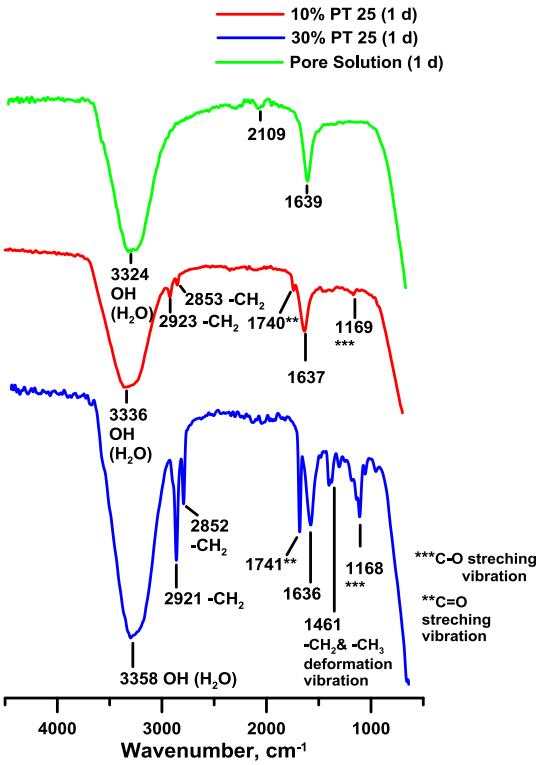
10% PT 25 (1 d)
30% PT 25 (1 d)
Pore Solution (1 d)
2109
1639
3324
OH
(H2O)
2853 -CH2
2923 -CH2
1740**
1169
***
1637
3336
OH
(H2O)
2852
-CH2
2921 -CH2
1741**
1636
1461
-CH2& -CH3
deformation
vibration
1168
***
3358 OH (H2O)
***C-O streching
vibration
**C=O
streching
vibration
4000
3000
2000
1000
Wavenumber, cm-1

b)

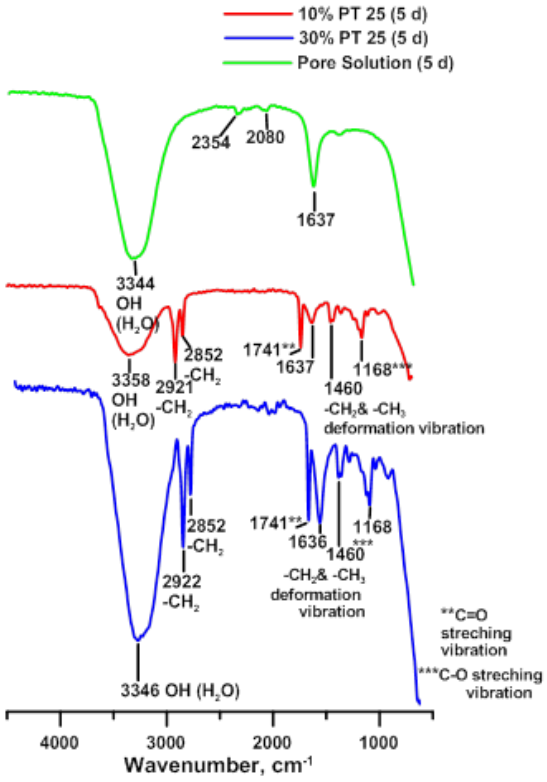
10% PT 25 (5 d)
30% PT 25 (5 d)
Pore Solution (5 d)
2354
2080
1637
3344
OH
(H2O)
3358
OH
(H2O)
2852
-CH2
2921
-CH2
1741**
1637
1168***
1460
-CH2& -CH3
deformation vibration
2852
-CH2
2922
-CH2
1741**
1636
1460
1168
***
-CH2& -CH3
deformation
vibration
3346 OH (H2O)
**C=O
streching
vibration
***C-O streching
vibration
4000
3000
2000
1000
Wavenumber, cm-1

c)

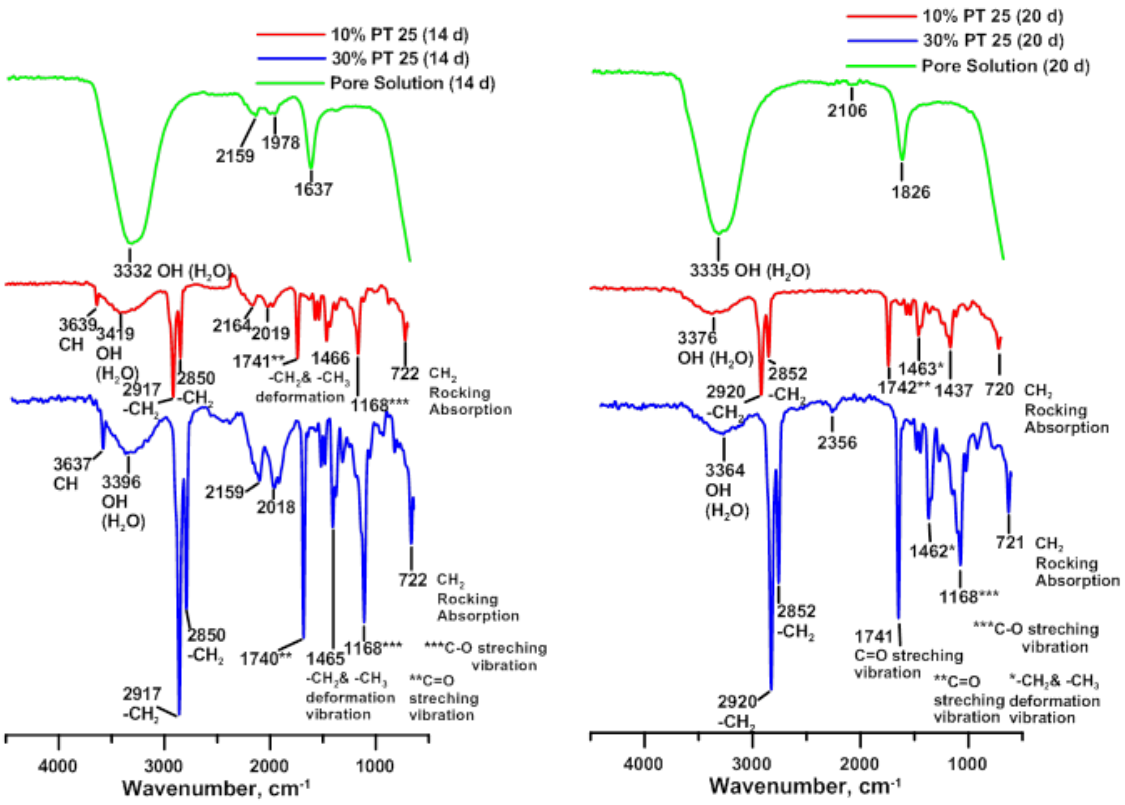

d) e)

Figure 0-12: FTIR Spectrum for a) pure PT; Pore Solution Mixes at b) 1 day, c) 5 days, d) 14 days, and e) 20 days

There are three peaks attributed to plain pore solution; 3324 cm^{-1}, 2109 cm^{-1}, and 1639 cm^{-1} at one day. The O-H bonds are represented by the wavenumber 3324 cm^{-1} and 1639 cm^{-1}. The peak around 3324 cm^{-1} shifts up in wavenumber for the mixes with PT 25, while the peak and the 1639 cm^{-1} peak shifts to a lower wavenumber when mixed with the PT 25. In addition as curing time increases the amplitude of the O-H peak at 1639 cm^{-1} drastically decreases, this can be attributed to (i) the sample of material tested not being homogenous, or (ii) an effect of crosslinking of the bonds. The crosslinking could then be related to the results from TGA thus causing the PT evaporation peak to shift into

a higher temperature range causing it to merge with the temperature range associated with dehydroxlization of $Ca(OH)_2$.

The peaks associated with the $–CH_3$ asymmetrical vibration cannot be detected at any age. The C-O and C=O stretching vibration peaks show no noticeable change with time.

At 5 days the $–CH_2$ and $–CH_3$ deformation vibration peak starts to be seen at a wave number of 1460 cm^{-1}. Over time this wavenumber is shifted up to 1466 cm^{-1} at 14 days, but by 20 days the wave number shifts back down to 1462 cm^{-1}. The $–CH_2$ and $–CH_3$ deformation vibration seems to stay stable overall in the mixes, while the $–CH_2$ functional group and the symmetrical vibration of $–CH_2$ shift upward in peak from the pure condition of 2915 cm^{-1} to approximately 2922 cm^{-1}, and 2847 cm^{-1} to 2852 cm^{-1}. The $–CH_2$ symmetrical vibration wavenumber does not change any with time, while the $–CH_2$ functional group sees a fluctuation in wave number with time.

Changes in the $–CH_2$ functional group can be due to the crosslinking affects as discussed in Section 5.5.

4.8.2 DSC

DSC was performed on the synthetic pore solutions at 3, 14 & 20 days. The purpose is to determine if and how the PT 25 is interacting with the synthetic pore solution and further, if there is a reduction in the thermal capabilities as seen with the directly mixed pastes.

There is an enthalpy peak occurring when the water in the pore solution undergoes phase change from solid to liquid during the heating cycle. The smaller peaks seen around $25^{o}C$ in the mixes with PT 25 are attributed with the phase change thermal properties. The following DSC scans cannot be accurately used to determine thermal efficiency. This is due the small sample sizes being unrepresentative of the mixture of pore solution and PT,

because as aging time continued at 14 and 20 days the PT began to precipitate into the pore solution and was unable to be mixed back as discussed previously. The following DSC scans then will be looked at for determination of if thermal degradation was occurring because of the pore solution as seen in the paste mixes DSC scans at 3 and 28 days.

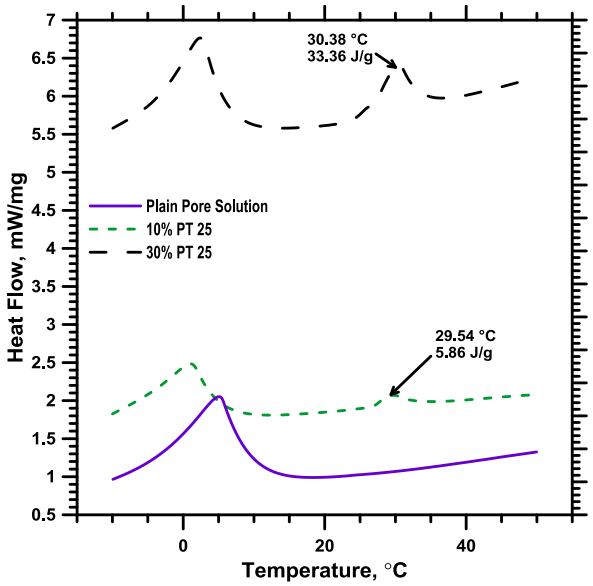

Figure 0-13: DSC heating and cooling scan of pore solutions at 3 days

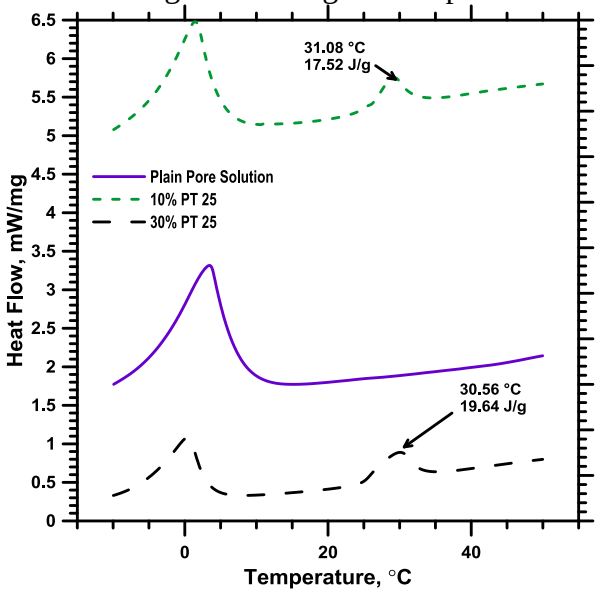

Figure 0-14: DSC heating and cooling scan of pore solutions at 14 days

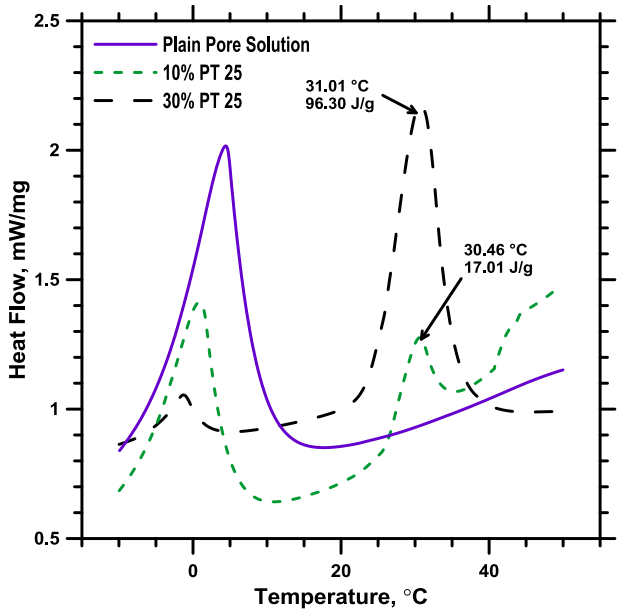

Figure 0-15: DSC heating and cooling scan of pore solutions at 20 days

The phase change temperature of the mixes with PT 25 increased to around 30^0C. This shift in phase transition shows that the thermal stability of the PT is increasing when mixed with the pore solution, thus allowing for a more thermally stable composite material that would cause the mass loss rates for evaporation of PT and dehydroxylation of $Ca(OH)_2$ to overlap as age increases over time.

This stayed consistent at all ages. The latent heat characteristics of the PT 25 remained even as the precipitate formed. This shows that enthalpy relaxation is not occurring due to pore solution interaction with PT in pastes, but this does not indicate that the physical nature of PT 25 is being changed as seen by the drastic shift in phase transition temperature and its appearance as an amorphous solid. These changes in PT material characteristics can play an increased role in the pressure and confinement effects discussed in Section 4.1.1. For instance: the amorphous PT is under increased pressures in the pores and thus experiences non-freezing layers at the interface of the paste matrix

[34], and an amount of the PT when confined may not be taking part in the phase transition and thus would cause a depression in the latent heat [55].

4.9 Summary

Direct incorporation of PCM into cement pastes poses many issues with the mechanical and chemical characteristics of both PCM and cement. Everything from the micro pore structure to the strength properties of the paste is altered in some way due to PCM integration. Strength decreases were attributed to the unhydrated cement particles becoming coated in PCM, which were unable to hydrate and could not be utilized as a nucleation surface. Pore volume intruded was higher at three days for PCM mixes because less hydration was occurring and the voids created by the water and PCM repulsing one another. Thermal characteristics of PCM-cement mixes were lower than the theoretical at 3 days, but practically nonexistent at 28 days, this is due to i) cross-linking of PCM with silica hydrates causing enthalpy relaxation, ii) physical effects caused from reduction in pore size, and iii) the formation of the semi-solid precipitate due to PT in the pore solution is changing the physical ability of the PCM to change phases completely in the pores. Reduction in heat flow was seen in isothermal testing from the addition of PCM, suppression in hydration peak and retardation of the acceleration were observed for all mixes with PCM. Reaction of the PCM in a synthetic pore solution was analyzed showing that the PCM is combining with the $Ca(OH)_2$ forming a thermally stable semi-solid material as seen by DSC scans, furthermore no chemical reactions between the pore solution and PT were noted from the FTIR spectra meaning the crosslinking was purely physical. Further analysis needs to be done in order to better understand the cross linking

of PCM with CSH and the interaction of PCM with pore solution. Direct incorporation of bulk PCM during mixing of cement should not be attempted without proper encapsulation for the following reasons: (i) drastic strength decrease, and (ii) thermal degradation of PCM in the system thus making the purpose behind incorporation of PCM into cementitious systems null.

INFLUENCE OF IMPREGNATION OF PCM INTO LIGHTWEIGHT AGGREGATES ON THERMAL AND MECHANICAL PROPERTIES OF MORTARS

5.1 Introduction

The goal of this chapter is to gain a better understanding of the mechanical and thermal changes occurring when PCM is incorporated then utilized in a cement mortar. DSC was a tool used for the effective absorption through thermal efficiency of the incorporated PCM in LWA. Testing on mechanical effects was executed using compressive strength testing to understand the strength development. Isothermal calorimetry was completed looking at the heat of hydration. Testing for thermal efficiency of the mortar mixes was done using a cylindrical thermal conductivity device. Finally FTIR analysis on the mortar samples was utilized for analysis of chemical bonding of the system when PCM is added.

5.1.1 Saturation Method

The first method considered for impregnation of PCMs into LWA materials was the use of saturation. The saturation methodology and sample preparation strategies were presented previously in Section 3.2.1. This method included 24 hours of atmospheric pressure saturation and a 2 hour vacuum saturation method followed by 24 hours of saturation in atmospheric conditions, with 24 hours of oven drying at various temperatures. Investigation of the absorption for each method includes DSC measurements of the samples after PCM saturation.

DSC measurements were performed on PCM saturated LWA sand samples to find the peak temperature of the phase change and enthalpy. Figure 5-1 below presents the results of the DSC study for PT 25 and PT 29 using the different saturation methods, as mentioned previously, and oven drying temperatures.

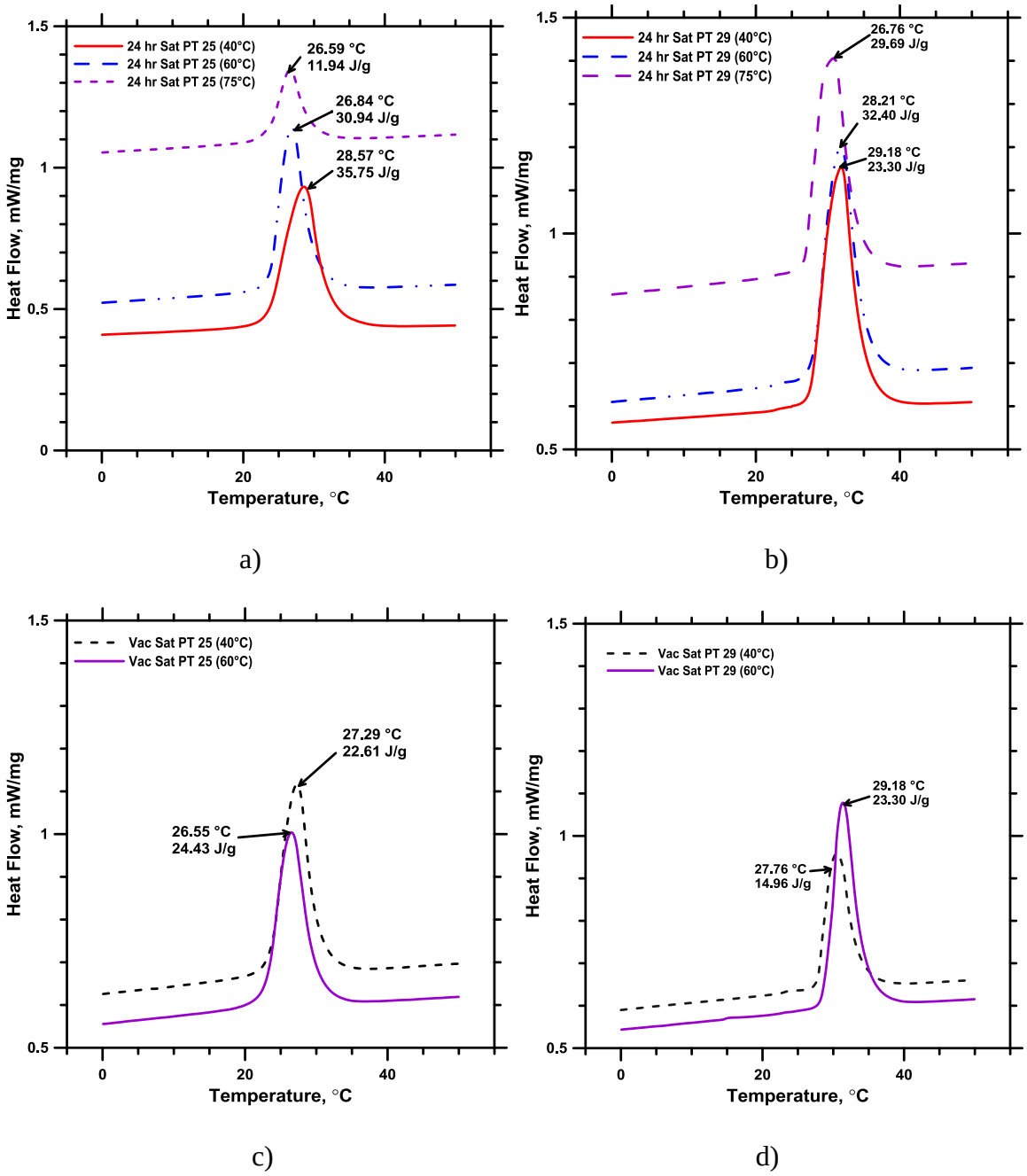

Figure 0-1: DSC heating and cooling scans for the 24 hr saturations methods using a) PT 25 & b) PT 29; vacuum saturation method for c) PT 25, & d) PT 29

PCM confinement in pores leads to a broader DSC signal, with a tail in the low temperature region that increases in size inversely with pore size [55]. This broadening in the signal pushes the onset temperature to a lower temperature but the phase change takes

place over a larger span of temperatures, and because of this behavior phase transition temperature will be considered the temperature at the maximum value of the peak for LWA-PCM composites and the onset transition of the phase change transition.

There is a notable shift in the phase change temperature between the LWA-PCM composites and the bulk PCM. PT 25 saturated LWA showed an increase in phase change temperature of 1 to 3°C and PT 29 saturated LWA showed a decrease of 1 to 3°C. Interactions between the pore surface and the PCM play a large role in change with phase transition range, this can be affected by i) physical means, such as pressure, and volume change and ii) physio-chemical means such as hydrogen bonding. When the PCM has strong interaction with the porous material the melting point will increase, conversely a weak interaction will reduce the phase change temperature [42]. Capillary forces between the PCM and lightweight aggregate pores can hinder movement of the PT chains during the solidification stage thus causing the PT to be amorphous while in its solid form rather than crystalline [57]. In addition, changes in phase transition can be attributed to the behavior of fluids changing phase in pores, which is dependent on the surrounding temperature and pressure, along with the geometry and the interaction with the crystal wall [42, 55, 58]. This behavior can be governed by the Clapeyron Equation (Equation 3):

$$\frac{\mathrm{dT}}{\mathrm{dp}} = \mathrm{T} \cdot \frac{\Delta_s^l \mathrm{V_m}}{\Delta_s^l \mathrm{H_m}} \tag{3}$$

The following relationships are true:

$$\frac{\mathrm{dT}}{\mathrm{dp}} \alpha\, \Delta_s^l V_m$$

$\frac{dT}{dp} \alpha \frac{1}{\Delta_s^l H_m}$

p α $\frac{1}{r}$ ∴ p is inversely proportional for the critical pore radius of the LWA (0.005µm)

p α 200 μm^{-1}

Where, T is melting temperature, p is pressure, and $\Delta_2^l V_m$ and $\Delta_s^l H_m$ are the volume and enthalpy change during solid to liquid phase change, respectively. Volume change for paraffin has been found to be 0.12 – 0.16 ml/g in bulk conditions [42] and enthalpy change respectively. dT/dp will also be positive and as the pressure increases the melting temperature would increase. The volume change of the PCM in the pores leads to an increase in pressure during phase transition from solid to liquid, which leads to an increase in the melting temperature [42].

Assuming $\Delta_2^l V_m$ = 0.14 ml/g for both PT 25 and PT 29 in the bulk state and $\Delta_s^l H_m$ is 165.17 J/g for PT 25 and 184.54 J/g PT 29, T is 25.44°C and 29.79°C for PCM-25 and PCM-29, respectively. Rate of temperature change with pressure can be calculated by dT/dp = $T \frac{\Delta_s^l V_m}{\Delta_s^l H_m}$ results in 0.022°C/Pa for PT 25 (dT_{25}/dp) and 0.023°C/ Pa for PT 29 (dT_{29}/dp). As pressure increases the melting temperature would increase, this is assuming the PCM enthalpy and volume change are held constant.

Absorption plays an important role in the $\Delta_2^l V_m$ in a system; if a pore is filled more efficiently it will be subjected to a lower volume change from solid to liquid phase due to the confinement effect the pore walls impose, which will lead to a decrease in the dT/dp and thus decreasing the melting temperature. In addition $\Delta_s^l H_m$ is an inherent property of PCM which is considered to be held constant with the bulk PCM in pores such as LWA where no crosslinking is occurring.

PT 29 is less viscous during saturation allowing for better filling of the pores. This reduces the volume change during solid to liquid phase change also it has a larger enthalpy change than that of PT 25 thus attributes to the decrease in melting temperature as seen in the DSC results above.

Similarly, the Gibbs-Thomson equation (Equation 4) also states that the melting temperature will increase as pressure increases. When a liquid is confined in a small pore the surface becomes large compared to the volume and thus the contribution that interfacial surface free energy plays on the melting/solidification process. This is because an increase in the pressure inside the crystal caused by its curvature will create elevated melting temperatures as the crystal-wall interaction energy is lower than that of the liquid-wall energy [50].

$$\Delta Tf = Tpore - Tbulk = -\frac{2(\sigma_{SW}-\sigma_{LW})T}{H\rho R} \quad (4)$$

Where, ΔT_f is the change of the freezing or melting temperature of the confined liquid or solid respectively. The interfacial free energies for solid-wall and liquid wall interfaces are σ_{SW} and σ_{LW} respectively. Melting enthalpy is H (considered a constant bulk property for PCM), confining pore radius is R, and density of the solid is ρ (bulk property of PCM (0.85 g/ml)), temperature is T. The phase transition temperature of a solid to a liquid in a pore increases when the liquid-wall interfacial energy is higher than the free energy associated with the solid-wall interfacial energy, and vice versa [50]. This implies that the crystals confined in the pores are more stable than the liquid above the melting point associated with the bulk material being that the crystal could nucleate and grow from the pore walls [55]. In addition pressure effects are included because the radius of the confining pore is inversely proportional to pressure as discussed above. As the

confining radius becomes smaller the pressure will increase thus contributing to the increase in melting temperature. Paraffin PCMs have inactive molecule groups, $-CH_2$, and $–CH_3$, which are believed to cause no strong attractive forces between the paraffin and the inner surface of the porous material [42]. This affects surface effects so when surface amount is higher than volume the surface free energy will take precedence, and because paraffin is primarily inactive, typically leading to a depression in the phase change temperature of the paraffin in the porous medium [59]. If the pressure effects are not drastic enough due to reduced change in PCM volume or increase in pore radius then the physical effects described by Clapeyron and Gibbs-Thompson will not govern.

After oven drying at all temperatures for 24 hours it was determined by visual inspection that all sand samples had a layer of PCM left on the surface as shown in Figure 5-2 indicated by the darker color, and spotting of white wax. This surface coating could pose an issue of interference with hydration as well as poor bonding with the cement paste [60].

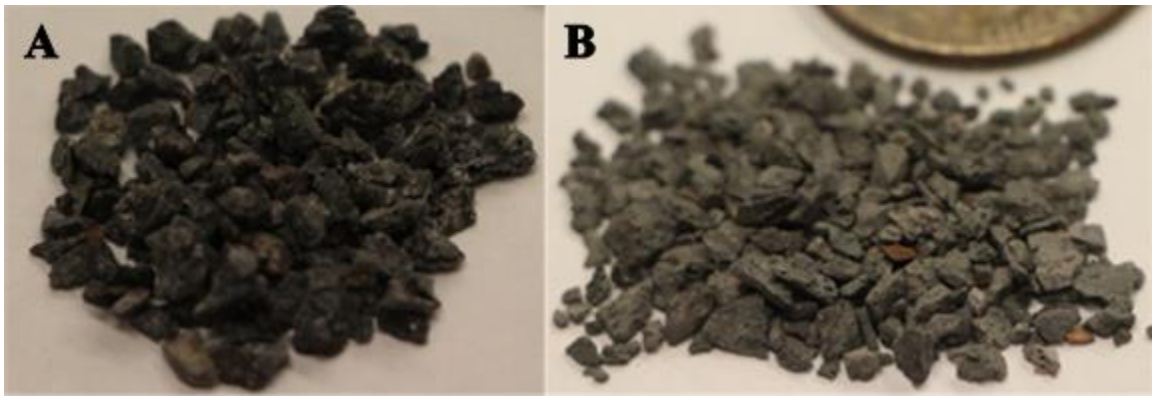

Figure 0-2: Picture of A) PCM saturated LWA, B) plain LWA

Based upon this, it is clear that the adsorption percentages determined using DSC may not be accurate, as it would include the PCM that remains on the surface of the sample. In practice, further measures would need to be taken to ensure encapsulation of the PCM into the LWA to avoid possible mechanical performance disadvantages associated with PCM being present on the surface of the fine aggregate. Furthermore, based on the apparent impractically of eliminating all the PCM from the surface of the fine aggregate, further investigation of the saturation methods were completed with the intent of providing a fine coat of cement paste on the PCM-LWA composite to eliminate the exposure of surface PCM to the structural cement paste.

The effective absorption of the PCM was calculated by using the ratio of the enthalpy of the pure PCM to the enthalpy of the impregnated aggregate. These results are tabulated in Table 5-1.

Table 0-1: Phase change temperature (onset temperature for pure PCM & peak temperature for PCM-LWA composites), enthalpy and PCM absorption for each saturation method and temperatures (32°C/40°C is 32°C saturation temperature with a 40°C oven drying temperature)

Pure PCM		Vacuum Saturation		24-hr Saturation		
PT 25		32°C/40°C	32°C/60°C	32°C/40°C	32°C/60°C	40°C/75°C
Enthalpy (J/g)	165.17	22.61	24.43	35.75	30.94	11.94
Effective Absorbed (%)	100	13.69	14.79	21.64	18.73	7.23
PT 29		32°C/40°C	32°C/60°C	32°C/40°C	32°C/60°C	40°C/75°C
Enthalpy (J/g)	184.54	14.96	23.3	31.9	32.4	29.69
Effective Absorbed (%)	100	8.11	12.63	17.29	17.56	16.09

Absorption and retention of PCM in porous materials is dependent on a variety of factors, such as the pore structure, temperature of the material, the liquid viscosity of the PCM, duration of immersion, surface area of material, liquid pressures, pre-existing moisture, and polarity of PCM [32]. Viscosity varies inversely with temperature; the viscosity must be low enough to allow absorption but high enough to prevent storage loss when the material is taken out of the liquid PCM or oven dried. The 24 hour saturation method iii (saturation at 40°C and oven drying at 75°C) had the lowest effective absorption when compared to the other 24 hour saturation methods; this can be attributed to the oven temperature being above the optimal temperature allowing for PCM to flow out of the pores, for this reason this method was not considered further for use in the coating method.

The vacuum methods using oven drying temperatures of 40°C and 60°C had lower absorption percentages than their counterparts for the 24 hour saturation method only. The vacuum duration of 2 hours did not lead to a significant increase in the thermal efficiency. This indicates that the vacuum saturation at a time of 2 hours has very little influence on absorption. There is a combination of affects that could be causing issues with the effectiveness of the vacuum saturation such as (i) the hot plate heating source was not consistent enough to allow temperature of the PCM to remain constant temperature, thus allowing solidification to occur on the top layer (this was observed affect but could not be mitigated with consistence via a hot plate), and (ii) the 2 hour vacuum duration did not allow proper evacuation of air from the pores. Further investigation for a system that maintains the temperature in the vacuum would need to be done in order to improve the reliability and repeatability of the testing. The samples had

the closest effective absorption to the expected value of 12% as calculated using ARIZ 211c method on the LWA. PCM was noticed to coat the surface of these samples also and would need to be subjected to a cement coating that would in further reduced the effective absorption (as determined using the thermal efficiency through enthalpy results). For this reason vacuum saturation was not further taken into consideration for the coating method.

A more in depth study of the 24 hour saturation was completed using three different oven drying temperatures (40^0C and 60^0C), with the saturation temperature held at 32^0C. The absorption difference between PT 29 at 40^0C and 60^0C is 0.27%, since the difference was negligible it was not analyzed further for determining the best saturation method to be coated. The oven drying temp at 40^0C for PT 25 had revealed a higher absorption capacity, which was attributed to a higher volume of surface coating of the LWA particles compared to those oven dried at 60^0C. Thus, the 24 hour ambient saturation method with an oven drying temperature of 60^0C was selected and used in further tests.

The difference in effective absorption of PT 25 and PT 29 can be attributed to the following affects: i) because PT 29 has less viscosity it was not retained within the pores, ii) the latent heat of the confined PT 29 is experiencing non-freezing layers at the interface of the LWA matrix [34], and iii) an amount of confined PT 29 may not be taking part in the phase transition and thus would cause a depression in the latent heat [55].

The second method considered for encapsulation of PCM in LWA materials was through the use of coatings. The methodology and sample preparation strategies were presented previously in Section 3.2.2.

The efficiency of the coating process on the thermal performance of these LWA materials was analyzed using DSC; the results of this analysis are presented in Figure 5-3. As above PCM absorption was determined by comparing the enthalpy of the pure PCM to the enthalpy of the impregnated aggregate, these results are presented in Table 5-2.

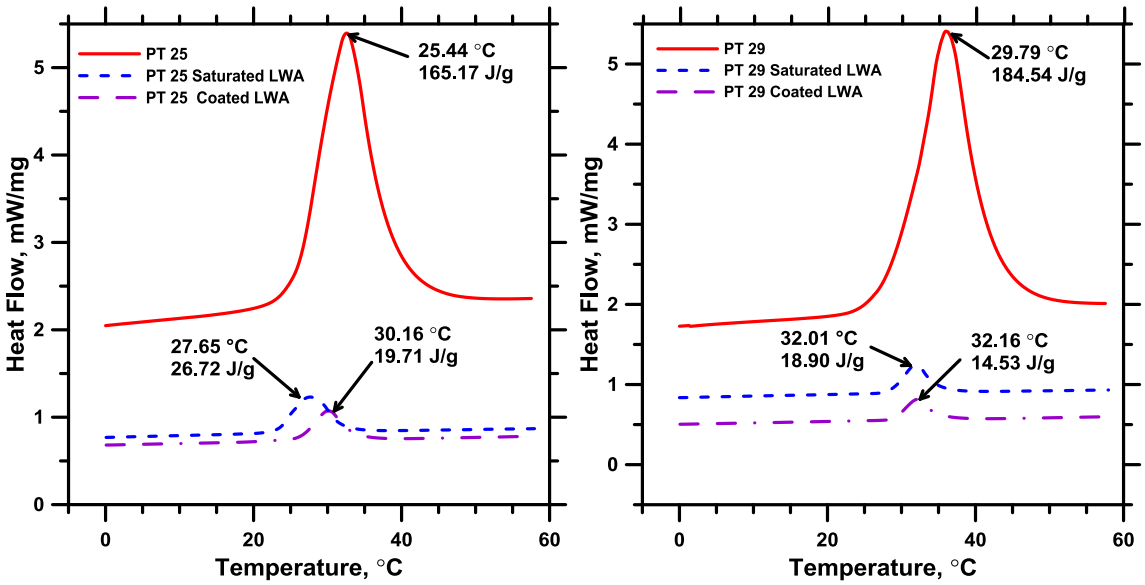

a) b)

Figure 0-3: Heating and cooling scan for a) pure PT 25, Saturated LWA, Coated LWA; b) pure PT 29, Saturated LWA, Coated LWA

The amount of PCM in the LWA is the same as the saturated sand, with a cement slurry coating added. This coating essentially reduces the enthalpy and thus the effective absorption based on the parameters set. The coated sand mixes reduced in enthalpy, from 26.72 J/g to 19.71 J/g for PT 25 and 18.90 J/g to 14.53 J/g for PT 29. This decrease in enthalpy is considered a decrease in effective absorption. The reduction in enthalpy can

be related to a number of different things: the volume of PCM is effectively reduced in the coated LWA material, and the surface coated with PCM is now experiencing confining effects the cement coating is imposing.

It can be noted that between the saturated LWA and the coated LWA there was an increase in the phase transition peak temperature. The increase in phase change temperature is attributed to the additional surface interaction through capillary forces [57]. Before the coating was applied the surface of the LWA had a thin layer of PCM, which was not subjected to the pore pressures and because the surface interaction was less the interfacial surface free energy was reduced. Once the coating was added the interfacial surface free energy increased causing the increase in pressure and thus increasing the pressure during phase change transition and thus according to Clapeyron equation (Equation 4) increase the melting temperature.

Table 0-2: Enthalpy and PCM absorption for saturated sand and coated sand

	Pure PCM	Saturated Sand	Coated Sand
PT 25		**24 hr (32°C/60°C)**	**w/c 0.75**
Enthalpy (J/g)	165.17	26.72	19.71
Effective Absorbed (%)	100	16.18	11.93
PT 29		**24 hr (32°C/60°C)**	**w/c 0.75**
Enthalpy (J/g)	184.54	18.9	14.53
Effective Absorbed (%)	100	10.24	7.87

Large batches of saturated LWA and coated saturated LWA were made using PT 25 and PT 29. Three samples were tested with DSC and the enthalpy results (as shown in Table

5-2) were averaged and used to determine the percentage by volume of PCM for the batches that would be used in the mix design.

All PCM percentages were accounted for in the 50% sand volume, with the paste volume fraction remaining constant. The amount of PCM to be added was set to 11.93% for PT 25 and 7.87% for PT 29. For coated LWA mixes complete replacement of LWA was done, creating a PCM percentage by volume of 5.97% and 3.94% for PT 25, and PT 29, respectively. PCM volume was to be held constant for all mixes to the above percentages of 5.97% (PT 25) and 3.94% (PT 29) and since complete replacement of LWA with saturated LWA would have a larger PCM percentage, the replacement of LWA with saturated LWA volume was reduced to correspond with the set PCM volumes. Partial replacement was done at the following amounts, 38.4% PT 29 saturated LWA and 36.9% PT 25 saturated LWA with the remaining percentages made up of plain LWA giving the mortar a total LWA volume fraction of 50%.

Figure 0-4: Picture of coated LWA

Pictured in Figure 5-4 is a sample of coated sand. Through the coating process some individual aggregates agglomerated with adjacent particles creating a different gradation of LWA that could potentially influence characteristics observed in the testing results of

the mortars. These connected individual aggregate particles will create a new matrix that could affect the thermal conductivity.

5.2 Mechanical Effects of PCM in Mortar

Compression tests were completed at ages of 3, 14 and 28 days, for each mix. The mixes that were tested are as follows; OPC, PT 25 Saturated LWA, PT 25 Coated LWA, PT 25 direct addition 5.97%, PT 29 Saturated LWA, PT 29 Coated LWA, PT 29 direct addition 3.94%.

All mixes with PT 25 or PT 29 showed a lower strength than the control mix. It is a well-known fact that PCM does interact with C-S-H formation thus reducing strength [20, 24, 33]. PCM also reduces the peak hydration temperature of the cement, controlling thermal stresses and cracking which would help for long term strengths, but reducing the peak hydration will affect the early age strength [24].

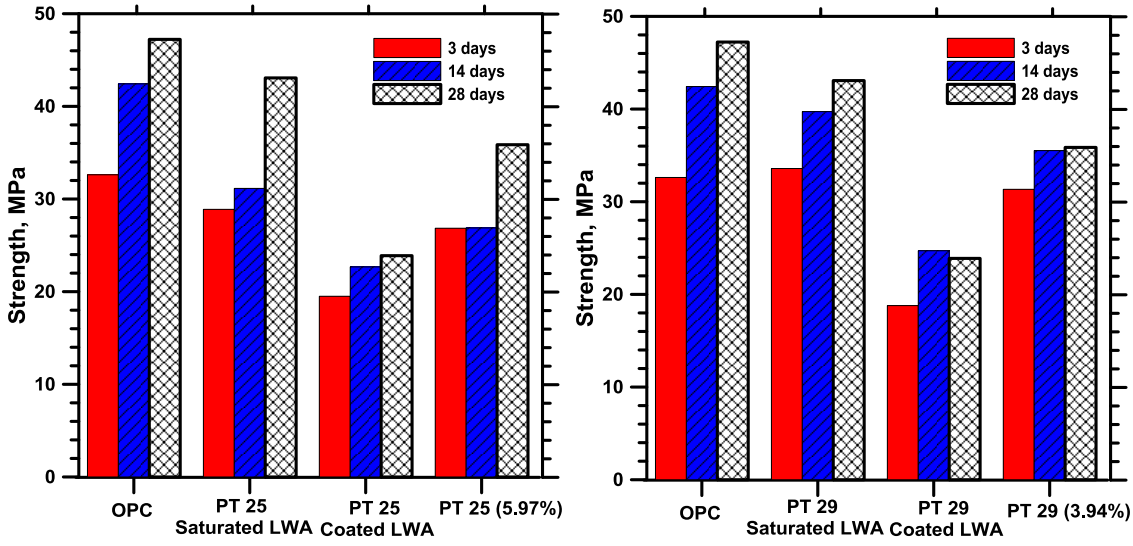

Figure 0-5: Compression strengths a) PT 25 mixes, b) PT 29 mixes

The PT 25 saturated LWA and the direct addition PT 25 (5.97%) had similar 3 day strengths, with an approximate 11% and 18% decrease respectively in strength compared

to the OPC mix. The PCM saturated LWA exhibited greater strengths than that of the 50% coated PCM saturated LWA. This can be attributed to the plain LWA and the saturated LWA being mixed thoroughly. This can allow for nucleation on the unsaturated sand surfaces.

The coated sand mixes had substantially lower 3 day strength in comparison to OPC, with a 40% decrease. Both coated LWA mixes yielded the lowest strengths along with the lowest strength development over time. This effect can be attributed to three possible causes (i) the use of the coating effectively decreases the volume of sand and increases the paste volume fraction, (ii) the localized high w/c ratio paste on the interface between the fine aggregate and the normal paste of the concrete results in a weak interface, increasing the likelihood of fracture, and (iii) the slurry coating fractured or PCM has absorbed through thus exposing PCM into the system causing paste-aggregate interfacial issues [33] along with reducing the surfaces for nucleation. A combination of these possible causes could be the reason for the large decrease in strength.

The direct addition of PT 25 and PT 29 displayed strength decreases due to the interaction of liquid PCM directly mixed with cement paste that can cause interference with hydration and bonding issues with the paste and aggregates [33]. Strength reduction is also due to the long chains of PCM wrapping around cement particles that cannot react to water [47] in addition to these cement particles unable to react they cannot be used as a nucleation point. Direct addition in mortars showed a higher strength than coated aggregate because the volume of PCM was small and PCM could coat sand particles or

cement particles thus reducing the PCM coated cement particle, while uncoated sand particles could be used for nucleation.

PT 25 had a higher volume fraction than PT 29 and thus a larger decrease in strength, indicating that when more PCM is in the mix the more adversely it will affect it.

5.3 Investigation of Heat Evolution of Mortars

Isothermal calorimetry monitors the heat evolution which is related to the degree of hydration since because C_3S and C_3A have a high exothermic release of energy at -137.6 kJ/mol and -248.3 kJ/mol respectively, while the heat release in the formation of C-S-H is quite low (-20 kJ/mol) [30]. Cumulative heat release and the heat flow for each mix was recorded over a 24 hour period, as shown in Figure 5-6. The dissolution peaks as seen in the first few minutes is due to the rapid heat release that occurs when the cement minerals are dissolving and reacting with water to form the amorphous layer of hydration product around the particles, thus keeping the particles from further reacting.

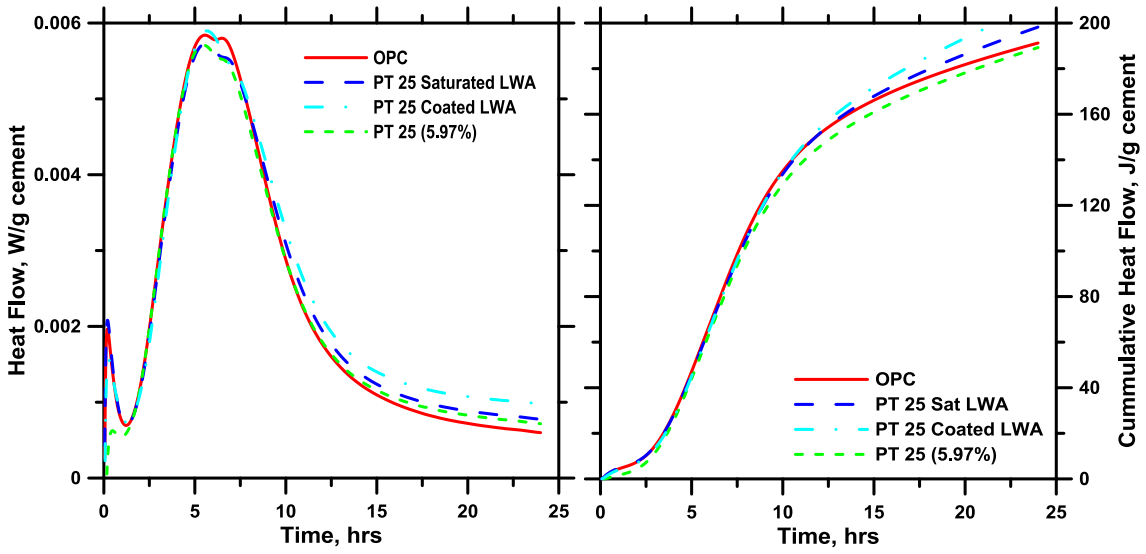

a)

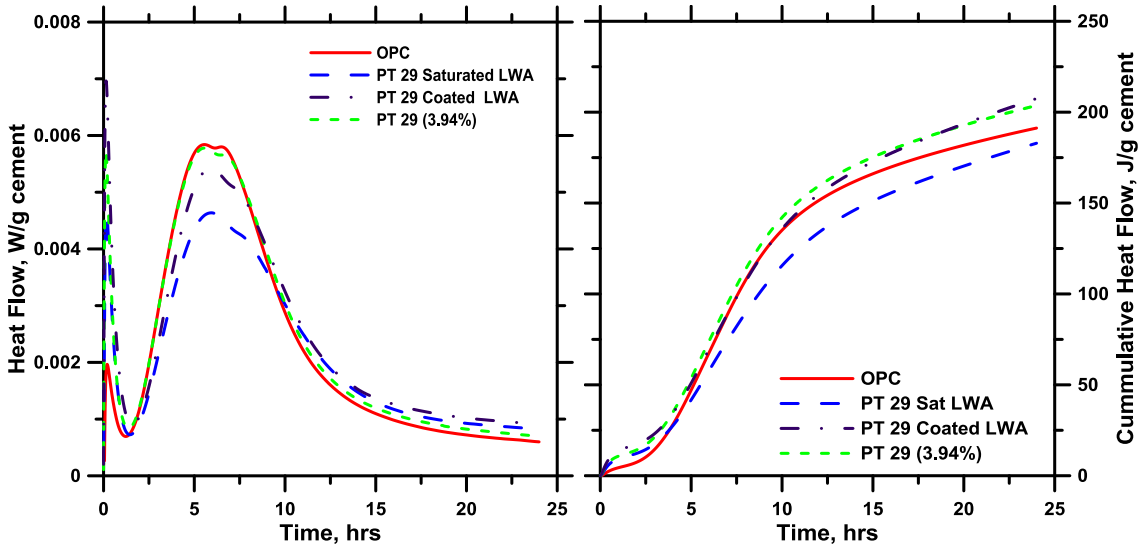

b)

Figure 0-6: Isothermal Conductivity heat flow and cumulative heat flow for a) PT 25 mixes, and b) PT 29 mixes

All plotting was done versus gram of cement binder in the system, which was held constant for all mixes. The acceleration period is when C_3S is hydrating and the rate of hydration is controlled by the rate of nucleation and growth of the hydration products. From the above graphs it is determined that the effects of PT 25 on the acceleration the binder system is slight with no apparent retardation occurring, though there is a suppression in the maximum heat flow and an extension of the deceleration period. On the other hand the mixes with PT 29 demonstrate larger effects on the binder in both acceleration and hydration. Retardation of the acceleration period is seen for the coated and saturated LWA mixes of approximately, ½ hour. Hydration suppression was also experience but at a greater extent than the mixes using PT 25.

PT 25 coated sand mix did not experience any apparent suppression, due to the effectiveness of the coating on the LWA. The saturated LWA and direct addition PCM-25 mixes experienced a greater suppression because the PCM on the surface of the

saturated LWA and directly added in were in direct contact with cement particles, thus interfering in hydration.

PT 29 mixes are showing greater affects to the binder in the system due to the viscosity of PT 29, more leakage is occurring from the LWA allowing for more PCM interaction with the cement binder in the system. Directly incorporated PT 29 should the least retardation when compared to PT 25 direct addition and all other PT 29 mixes, this is attributed to the volume of PCM being smaller than PT 25 and PCM coating of cement particles is reduced by the introduced sand volume. The saturated sand mix for PT 29 had the greatest suppression in heat flow due to the direct contact PCM on the surface of LWA had with the binder of the system.

5.4 Thermal Efficiency of Cylindrical Mortar Samples

Thermal conductivity of the mortars was tested over a six hour period using an apparatus developed at Arizona State University as discussed in Section 3.3.4. Thermal conductivity ratio is plotted against inner radius temperature at every 1/2 hour as shown in Figure 5-7.

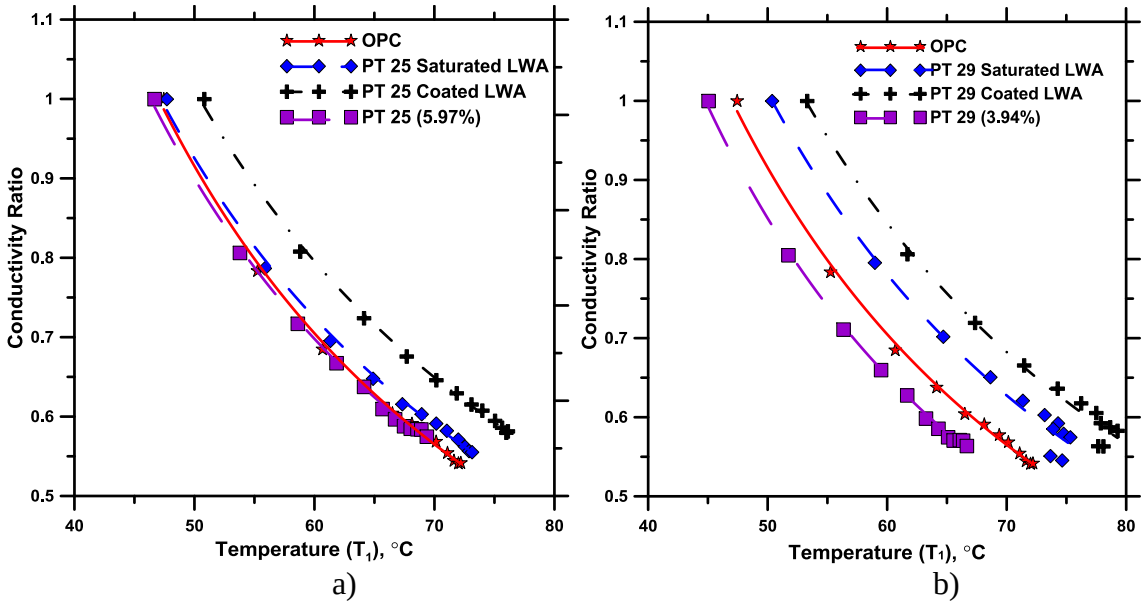

Figure 0-7: Thermal Conductivity ratio in relation to temperature for a) PT 25 mixes and b) PT 29 mixes

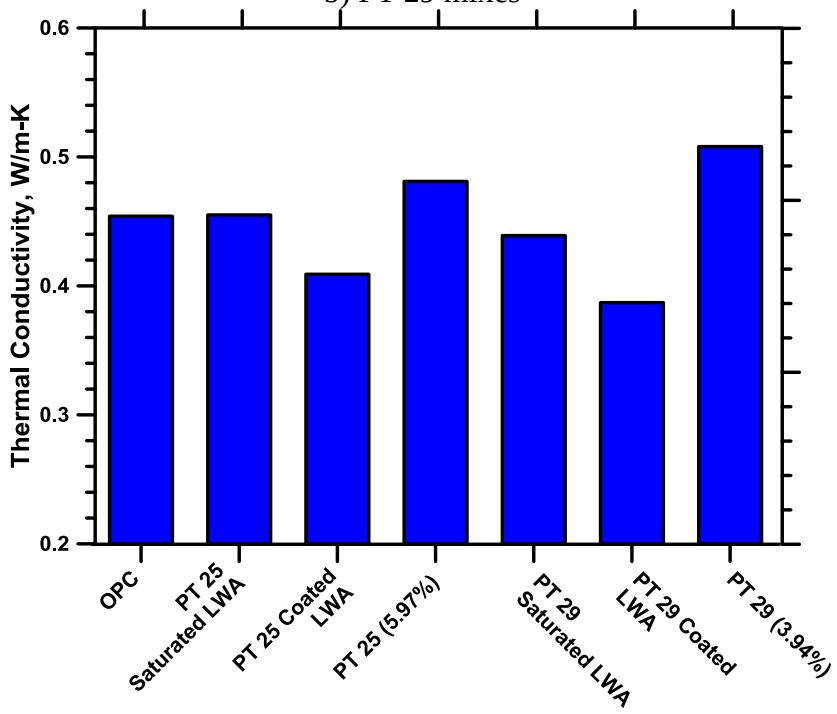

Figure 0-8: Thermal Conductivity results for all mortar mixes

There are multiple affects to thermal conductivity of a material such as mortars. Thermal conductivity is independent of curing age, but dependent on volume fraction of

aggregates, water cement ratio, admixtures, temperature and moisture conditions [61]. Pore structure of the mortar along with the phase change temperatures of the PCM affects the thermal conductivity [42]. The lower thermal conductivity of paraffin PCM does not allow the PCM to work as efficiently as discussed in Section 2.1.1, but the higher thermal conductivity of LWA can allow the PCM to be efficiently utilized [62].

The OPC mortar had a thermal conductivity of 0.45 W/m-K which is within the range expected for a lightweight concrete [41]. PT 29 coated LWA had the lowest thermal conductivity of 0.387 W/m-K. All direct addition PT mixes had thermal conductivity higher than OPC mortar.

The decrease in thermal properties of the direct addition PCM can be attributed to (i) PCM in direct addition is not mixed well in the mortar, and (ii) PCM is degrading in the cementitious system [20], thus being unproductive and (iii) changes in the aggregate volume could be affecting the thermal conductivity.

The PT 29 mixes with saturated LWA and coated LWA had a drop in thermal coefficient between 3 to 3.5 hours and 5 hours after which the coefficient increased and then stabilized. Within this window is when the PCM is at its latent heat storage capacity. Latent heat storage allows for heat to be stored without temperature rise in the material, thus the T_2 (outer radius temperature) would be reduced while T_1 (inner radius temperature, initiated by the heating cartridge) is increasing. This would lead to decrease in thermal conductivity. The time it takes for the latent heat storage capacity to be reached is dependent on the conductivity of the surround material, and the heat absorption of the PCM, if melting is occurring layer by layer there would not be a

substantial effect seen at a specific time. When the PCM is at its storage capacity it behaves like a sensible heat storage system, such that when it absorbs heat energy it increases in temperature, this is why an increase in T_2 is seen during the stabilized area. PCM incorporation is then most beneficial to offset the transfer of heat.

5.5 FTIR Results

FTIR testing was executed on all mortar mixes with PT 25 and PT 29. FTIR analysis was done to determine if chemical bonding was occurring between PCM and the hydration products. Pure PT 25 and PT 29 spectra depicted the same wavenumbers and so only the spectra from PT 29 mixes will be discussed below.

The FTIR spectra for PT 25 and PT 29 are presented in Figure 5-9.

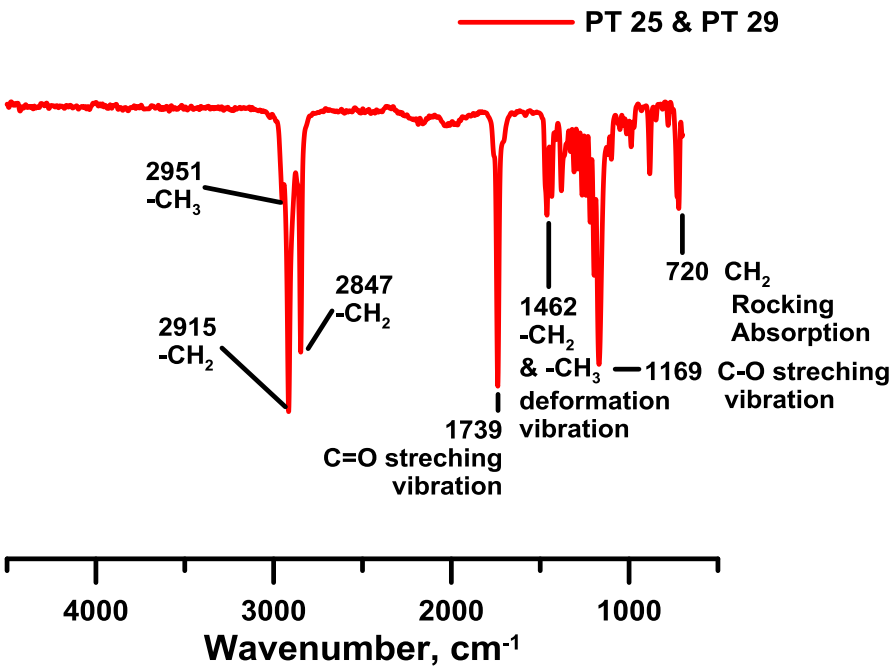

Figure 0-9: FTIR Spectrum for PT 25 & PT 29

All peaks appear below 3000 cm^{-1}, meaning PT25 and PT 29 are saturated hydrocarbons [42]. There are three peaks at the wave numbers of approximately 2953 cm^{-1}, 2915 cm^{-1},

and 2847 cm^{-1} corresponding to the asymmetrical vibration of the $–CH_3$ functional group, $-CH_2$ functional group and the symmetrical vibration of the $–CH_2$ functional group, respectively. The wavenumber around 1730 cm^{-1} is the stretching vibration of the carbon double bonded with oxygen. The peaks in the range at 1462 cm^{-1} for PT and 1467 cm^{-1} for Micronal correspond to the $–CH_2$ and $–CH_3$ deformation vibration. The single bond carbon – oxygen stretching vibration appear around the range of 1160 cm^{-1}. CH_2 rocking absorption band is represented by a wavenumber of 720 cm^{-1}. The $–CH_2$ peaks are more intense than the first peak representing $–CH_3$, signifying that there are more $-CH_2$ molecules than $–CH_3$. The FTIR spectrum for PT reveals that it has the same bonding present in paraffin.

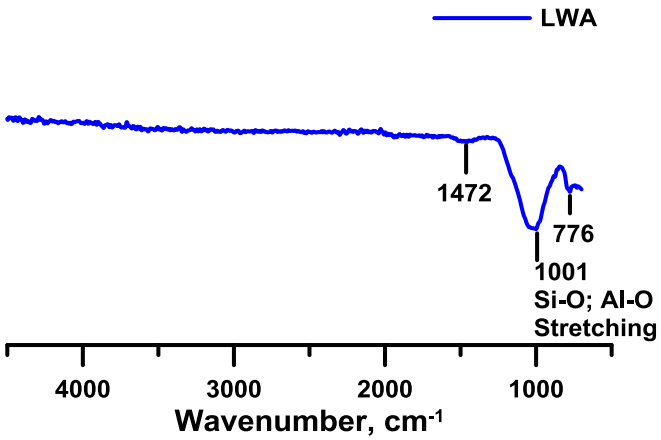

Figure 0-10: FTIR Spectra from Stalite LWA

The FTIR spectra for Stalite LWA indicated three distinctive peaks at 1472 cm^{-1}, 1001 cm^{-1} for Si-O and Al-O stretching, and 776 cm^{-1}.

The spectra for the OPC mortar at 14 days is shown in Figure 3-10 below, the peaks corresponding to calcium hydroxide at 3634 cm^{-1} and the sulfate products at 1650 cm^{-1}. O-H stretching is at 3414 cm^{-1}, carbonates at 1412 cm^{-1}, and the stretching bands for Si-O and Al-O at 969 cm^{-1}.

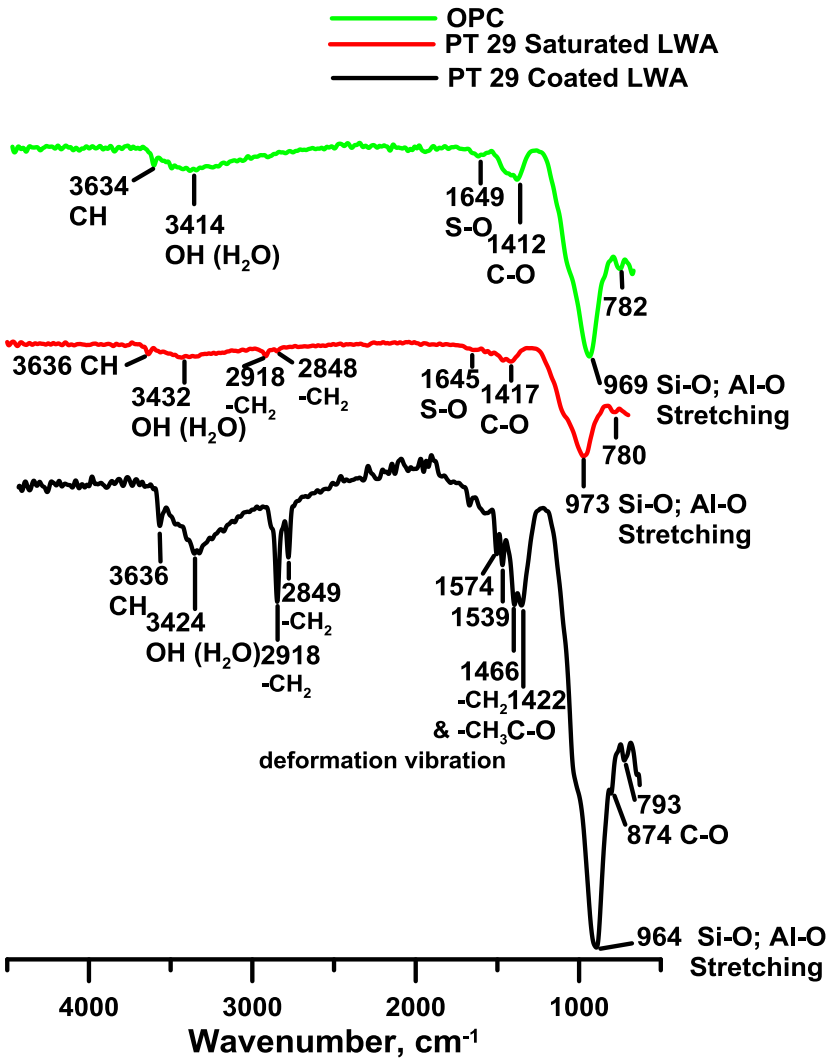

Figure 0-11: FTIR spectrum for PT 29 mixes at 14 days

Shifts in the Si-O-Si band can be attributed to the physical interactions between the confined PCM and the LWA matrix [63]. All high transmittance wavenumbers associated with PCM are still present implying chemical structure is remaining mostly unchanged. The wave numbers for CH, O-H stretching and carbonates, shifts higher when PCM is incorporated into the mortar. The wavenumbers corresponding to PCM that can be seen are shifted to a higher number in the mortar mix than that of the pure PCM. This shows that there is some change in the linear chain of PT 29 such that it is cross linking with

silica in the system. This cross linking is clearly physical in nature because no major new peaks are in the spectra indicating that there is no chemical reaction occurring [63, 64, 56].

A comparison of curing age on OPC mix and PT 29 coated sand mix for 14 and 28 days is presented in Figure 5-12.

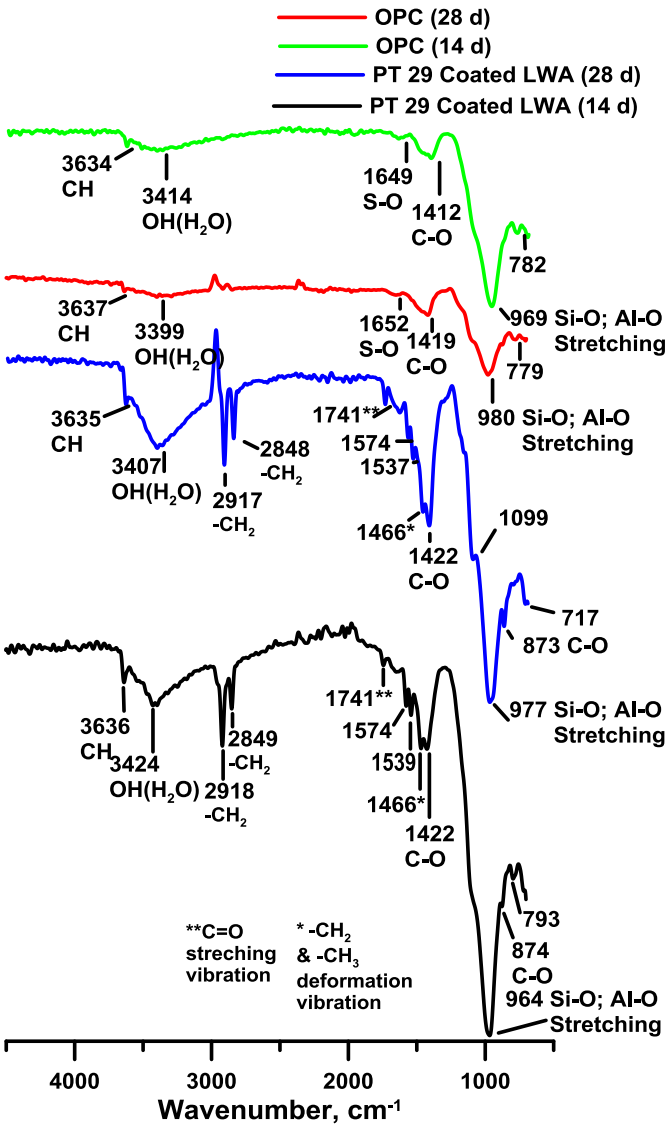

Figure 0-12: FTIR Spectrum OPC and PT 29 Coated Sand at 14 and 28 days

The shift that is seen to a higher wavenumber from 14 day OPC to 18 day OPC is interpreted as an increase in the silica polymerization in the gel [65]. The increased silica content can then contribute to the interaction of the paraffin with the matrix. The major peaks signifying PCM in the coated LWA mix are still present at 28 days and remain unchanged from 14 days. This would imply that the coated sand mix is effectively keeping the PCM from changing chemical bonds with age.

5.6 Summary

Incorporation of PCM in LWA to be utilized in mortars was studied in order to better understand the effects of PCM in concrete systems and to analyze the encapsulation capability of PCM in LWA. The straining system should be improved to reduce PCM left on the surface. Encapsulation in LWA did not resolve the issue of strength reduction with PCM incorporation. Furthermore, using a cement slurry coating actually reduced the strength, an effect that is attributed primarily to strength at aggregate-binder interfaces due to the high water/cement ratio of the coating. Utilizing a mixture of plain LWA and saturated LWA appears to diminish some of the strength reduction effects; however it will also reduce the thermal efficiency of the material. Isothermal calorimetry results confirmed that the interference with C_3S and C_3A is very minimal but still a reduction in hydration rate was seen. These results also illustrated that while the PT is introduced into the LWA volume it can still directly interfere with hydration process via chemical means and through the thermal nature of the PCM. Thermal conductivity showed that mixes using PCM in LWA proved to be more thermally efficient while mixes with PCM directly added were less efficient, a result that is attributed primarily to interaction

between the PCM and paste. FTIR spectra illustrated that the PCM and the mortar were not interacting chemically to form new compounds, but shifts in the wavenumbers corresponding to PT and cement hydration indicates physical interactions. Silica polymerization over time occurs as indicated by the increase in wavenumbers, indicating C-S-H formation is continuing at later ages. LWA is a potential encapsulation method for PCM in concrete systems, further work needs to be done to improve techniques, reducing PCM leakage, and further understanding chemical affects PCM has on cement.

CONCLUSIONS

The purpose of this research was to investigate the influence phase change materials make in cementious systems. Mechanical, physical and thermal properties were analyzed as was the thermal performance of the PCM in the system. The first set of experiments were one to look at incorporation of bulk PCM into lightweight aggregate which would then be used in the mortar mixes. Compressive strengths, heat of hydration and thermal conductivity were tested of the mortars. The goal was to see if and how containment in the LWA was affecting PCM interaction with the cement. The second set of experiments were to analyze the effects of PCM directly incorporated with OPC pastes. The compressive strengths, pore structure, heat of hydration, hydration product formation, thermal characteristics, and interaction with pore solution were studied to better understand how the PCM interacts with the OPC directly.

6.1 Conclusions for PCM interaction with cement paste

- Mixing must be done using certain water:cement ratios along with certain additional volumes of PCM, such that the mix can remain homogenous. Mixes with w/c 0.7 and PCM volume 30% or greater were not accomplished due to large liquid to powder ratio.
- The pore structure of the paste was changed with PCM incorporation such that intruded volume of Hg was increased and threshold pore sizes were larger for larger percentages of PCM.
- Heat of hydration is affected substantially from the PCM in the paste, retardation and suppression in the hydration peaks were occurring.

- Thermal degradation of PT in the pastes due to crosslinking with silica hydrates leading to enthalpy relaxation
- Physical interaction of PT in pores and synthetic pore solution causes inefficient melting of the PCM in the pore.

6.2 Conclusion on encapsulated PCM in LWA for mortar mixes

- Encapsulation through a cement slurry coating caused lower strengths.
- Compressive strengths continue to be effected adversely even with PCM encapsulate into LWA, though mixes with partial saturated sand and plain sand seemed to fair more well.
- Heat of hydration is not as widely affected when PCM is encapsulated into LWA.
- Thermal Conductivity of the mortar mixes is improved with PCM in LWA then added in addition.
- FTIR spectra showed that there is a slight shift seen in the wavenumbers for PCM and the mortar with time, this is due to the higher formation of Silica in the system.

6.3 Recommendations for Further Work

Results from these experiments in this study show that thermal enhancement is possible through incorporation of phase change materials into lightweight aggregate or other encapsulation methods, while direct mixing application of bulk PCM causes large thermal reductions to occur, thus the thermal efficiency is diminished. Mechanical properties of cementious system were adversely affected in both cases of encapsulation and direct addition. There is an interesting phenomenon that occurred as seen in the study

of the interaction PCM had with the pore solution in the system that inadvertently changed some inherent properties of the PCM.

Further research is suggested as follows:

- Development of better batching techniques for saturating and coating LWA thus to reduce the time involved in making enough material and increasing the homogeneity of the saturation process.
- Scanning electron microscopy analysis of mortar mixes with and without the use of the cement slurry coating would help shed more light on the physical picture of strength loss seen in the coated sand mixes.
- Further chemical analysis on PCM interaction with cement paste products needs to better understand the effect of cross linking between cement particles and paraffin that is causing enthalpy relaxation.
- The interaction of PCM with pore solution needs to be further analyzed in order to see if crosslinking is forming with the $Ca(OH)_2$ in the pore solution and if that is causing a precipitate to form.
- Developing numerical modeling of heat transfer and efficiency of building systems using PCM incorporated into LWA.

REFERENCES

[1] Federal Research and Developement Agenda for Net Zero Energy, "High Performance Green Buildings," National Science and Technology Council (NSTC), 2008.

[2] S. G. Manari, *Thermal Response Of Cementious Systems Incorporating Phase Change Materials,* unpublished results.

[3] R. Baetens, B. P. Jelle and A. Gustavsen, "Phase change materials for building applications: A state-of-the-art review," *Energy and Buildings,* vol. 42, pp. 1361-1368, 2010.

[4] A. Carbonari, M. De Grassi, C. Di Pema and P. Principi, "Numerical and experimental analyses of PCM containing sandwhich panels for prefabricated walls," *Engergy and Buildings,* vol. 35, no. 5, pp. 472-483, 2006.

[5] K. Darkwa and P. W. O'Callaghan, "Simulation of phase change drywalls in a passive solar building," *Applied Thermal Engineering,* vol. 26, no. 8-9, pp. 853-858, 2006.

[6] B. M. Diaconu and M. Cruceru, "Novel concept of composite phase change material wall system for year-round thermal energy savings," *Engergy and buildings,* vol. 42, no. 10, pp. 1759-1772, 2010.

[7] H. E. Feustel and C. Stetiu, *Thermal Performance of Phase Change Wallboard for Residential Cooling Application,* Berkeley, CA: Lawrence Berkeley National Laboratory, 1997.

[8] T. Stoval and J. Tomlinson, "What are the potential benefits of including latent storage in common wallboard?," *Trans ASME,* vol. 117, pp. 318-325, 1995.

[9] R. Kedl and T. Stovall, Activities in support of the wax-impregnated wallboard concept: thermal energy storage researches activity review, New Orleans, Louisiana, USA: U.S. Department of Energy, 1989.

[10] F. Kuznik, J. Virgone and J. Noel, "Optimization of a phase change material wallboard for building use," *Applied Thermal Engineering,* vol. 28, no. 11-12, pp. 1291-1298, 2008.

[11] M. Li, Z. Wu and M. Chen, "Preparation and properties of gypsum-based heat storage and preservation material," *Energy and Buildings,* vol. 43, pp. 2314-2319, 2011.

[12] F. Kuznik, D. David, K. Johannes and J. J. Roux, "A review of PCM integrated in building walls," *Renewable and Sustainable Energy Reviews,* vol. 15, no. 1, pp. 379-391, 2011.

[13] C. Zhang, Y. Chen, L. Wu and M. Shi, "Thermal response of brick wall filled with phase change materials (PCM) under fluctuating outdoor temperatures," *Energy and Buildings,* vol. 43, no. 12, pp. 3514-3520, 2011.

[14] S. M. Hasnain, "Review on sustainable thermal energy storage technologies, Part I: heat storage materials and techniques," *Energy Conversion and Management,* vol. 39, no. 11, pp. 1127-1138, 1998.

[15] V. V. Tyagi, S. C. Kaushik, S. K. Tyagi and T. Akiyama, "Developement of phase change materials based microencapsulated technology for buildings: a review," *Renewable and Sustainable Energy Reviews,* vol. 15, no. 2, pp. 1373-1391, 2011.

[16] E. Osterman, V. V. Tyagi, V. Butala, N. A. Rahim and U. Stritih, "Review of PCM based cooling technologies for buildings," *Energy and Buildings,* vol. 49, pp. 37-49, 2012.

[17] H. Mehling and L. F. Cabeza, "Heat and cold storage with PCM," Springer-Verlag, Berlin, 2008.

[18] N. Neithalath and G. Sant, *Phase change materials in concrete: A new strategy to improve the thermal damage resistance and thermal energy efficiency of concrete structures, (unpublished results).*

[19] A. Pasupathy, R. Velraj and R. V. Seeniraj, "Phase change material- based building architecture for thermal management in residential and commercial establishments," *Renewable and Sustainable Energy Reviews,* vol. 12, pp. 39-64, 2008.

[20] D. W. Hawes, D. Banu and D. Feldman, "The stability of phase change materials in concrete," *Solar Energy Materials and Solar Cells,* vol. 27, pp. 103-118, 1992.

[21] A. Genovese, G. Amarasinghe, M. Glewis, D. Mainwaring and R. A. Shanks, "Crystallisation, melting, recrystallisation and polymorphism of n-eicosane for application as a phase change material," *Thermochimica Acta,* vol. 443, pp. 235-244, 2006.

[22] M. M. Farid, A. M. Khudhair, S. A. Razack and S. Al-Hallaj, "A review on phase change energy storage: materials and applications," *Energy Conversion and Management,* vol. 45, pp. 1597-1615, 2004.

[23] M. D. Romero-Sanchez, J. M. Rodes, C. Guillem-Lopez and A. M. Lopez-Buendia, *Phase Change Materials (PCMs) - Treated Natural Stone for Thermal Energy Storage in Buildings: Influence of PCM Melting Temperature,* Alicante, Spain.

[24] D. P. Bentz and R. Turpin, "Potential applications of phase change materials in concrete technology," *Cement Concrete Composites,* vol. 29, pp. 527-532, 2007.

[25] M. Hunger, A. G. Entrop, I. Mandilaras, H. H. Brouwers and M. Founti, "The behavior of self-compacting concrete containing micro-encapsulated Phase Change Materials," *Cement and Concrete Composites,* vol. 31, pp. 731-743, 2009.

[26] D. Hawes, D. Feldman and D. Banu, "Latent heat storage in building materials," *Energy and Buildings,* vol. 20, no. 1, pp. 77-86, 1993.

[27] N. Soares, J. J. Costa, A. R. Gasper and P. Santos, "Review of passive PCM latent heat thermal energy storage systems towards buildings' energy efficiency," *Energy and Buildings,* vol. 59, pp. 82-103, 2013.

[28] A. F. Regin, S. C. Solanki and J. S. Saini, "Heat transfer characteristics of thermal energy storage systems using PCM capsules: a review," *Renewable and Sustainable Energy Reviews,* vol. 12, pp. 2438-2458, 2008.

[29] D. Zhou, C. Y. Zhao and Y. Tian, "Review on thermal energy storage with phase change materials (PCMs) in building applications," *Applied Energy,* vol. 92, pp. 593-605, 2012.

[30] A. R. Sakulich and D. P. Bentz, "Incorporation of phase change materials into cementitious systems via fine lightweight aggregate," *Constructin and Building Materials,* vol. 35, pp. 483-490, 2012.

[31] L. F. Cabeza, C. Castellon, M. Nogues, M. Medrano, R. Leppers and O. Zubillaga, "Use of microencapsulated PCM in concrete walls for energy savings," *Energy and Buildings,* vol. 39, pp. 113-119, 2007.

[32] D. W. Hawes and D. Feldman, "Absorption of phase change materials in concrete," *Solar Energy Materials and Solar Cells,* vol. 27, pp. 91-101, 1992.

[33] D. W. Hawes, D. Banu and D. Feldman, "Latent heat storage in concrete. II," *Solar Energy Materials,* vol. 21, pp. 61-80, 1990.

[34] D. Zhang, Z. Li, J. Zhou and K. Wu, "Developement of thermal energy storage concrete," *Cement and Concrete Research,* vol. 34, pp. 927-934, 2004.

[35] T.-C. Ling and C.-S. Poon, "use of phase change materials for thermal energy storage: An overview," *Construction and Building Materials,* vol. 46, pp. 55-62, 2013.

[36] N. S. Berke and M. C. Hicks, "Electrochemical Methods of Determining the Corrosivity of Steel in Concrete," in *Corrosion Testing and Evaluation: Silver Anniversary Volume, ASTM STP 1000*, Philadelphia, Pa, American Society for Testing and Materials, 1990, pp. 435 - 440.

[37] L. Mammoliti, "Examination of the Mechanism of Corrosion Inhibition by Ca(NO2)2- and Ca(NO3)2- based Admixtures in Concrete," Waterloo, Ontario, Canada, 2001.

[38] K. A. Ismail and J. R. Henriquez, "Solidification of pcm inside a spherical capsule," *Energy Conversion & Management,* vol. 41, pp. 173-187, 2000.

[39] T. Hasenohrl, "An Introduction to Phase Change Materials as Heat Storage Mediums," in *Heat and Mass Transport*, Lund, Sweden, 2009.

[40] D. Morris, Development of Enhanced Cylindrical Specimen Thermal Conductivity Testing Procedure, (unpublished results).

[41] T. S. Yun, Y. J. Jeong, T.-S. Han and K.-S. Youm, "Evaluation of thermal conductivity for thermally insulated concretes," *Energy and Buildings*, vol. 61, pp. 125-132, 2013.

[42] D. Zhang, S. Tian and D. Xiao, "Experimental study on phase change behavior of phase change material confined in pores," *Solar Energy,* vol. 81, pp. 653-660, 2007.

[43] N. H. Atahan, O. N. Oktar and M. A. Tasdemir, "Effects of water-cement ratio and curing time on the critical pore width of hardened cement paste," *Construction and Building Materials,* vol. 23, pp. 1196-1200, 2009.

[44] A. B. Abell, K. L. Willis and D. A. Lange, "Mercury Intrusion Porosimetry and Image Analysis of Cement-Based Materials," *Journal of Colloid and Interface Science,* vol. 211, pp. 39-44, 1999.

[45] R. F. Feldman, *American Ceramic Society*, vol. 67, no. 30, 1984.

[46] D. Morris, Development of Enhanced Cylindrical Specimen Thermal Conductivity Testing Procedure, (unpublished results).

[47] D. P. Bentz, K. A. Snyder, L. C. Cass and M. A. Peltz, "Doubling the service life of concrete structures. I: Reducing ion mobility using nanoscale viscosity modifiers," *Cement & Concrete Composites,* vol. 30, pp. 674-678, 2008.

[48] C. A. Leon, "New perspectives in mercury porosimetry," *Advances in Colloid and Interface Science,* Vols. 76-77, pp. 341-372, 1998.

[49] R. A. Cook and K. C. Hover, "Mercury porosimetry of hardened cement pastes," *Cement and Concrete Research,* vol. 29, pp. 933-943, 1999.

[50] P. Maheshwari, D. Dutta, S. K. Sharma, P. K. Pujari, M. Majumder, B. Pahari, B. Bandyopadhyay, K. Ghoshray and A. Ghoshray , "Effect of interfacial hydrogen bonding on the freezing/melting behaviour of nanoconfined liquids," *Journal of Physical Chemistry C,* vol. 114, pp. 4966-4972, 2010.

[51] S. Montserrat, P. Cortes, Y. Calventus and J. M. Hutchinson, "Effect of crosslink length on the enthalpy relaxation of fully cured epoxy-diamine resisns," *Journal of Polymer Science: Part B: Polymer Physics,* vol. 38, pp. 456-468, 2000.

[52] G. Adam and I. H. Gibbs, "On the temperature dependence of cooperative relaxation properties in glass-forming liquids," *Journal of Chemical Physics,* vol. 43, pp. 139-164, 1965.

[53] N. M. Alves, J. L. Gomez Ribelles and J. F. Mano, "Enthalpy relaxation studies in polymethyl methacrylate networks with different crosslinking degrees," *Polymer,* vol. 46, pp. 491-504, 2005.

[54] D. Dondi, A. Buttafava, A. Zeffiro, L. Conzatti and A. Faucitano, "The role of silica in radiation induced grafting and crosslinking of silica/elastomers blends," *Polymer,* vol. 53, pp. 4579-4584, 2012.

[55] G. Dosseh, Y. Xia and C. Alba-Simionesco, "Cyclohexane and benzene confined in MCM-41 and SBA-15: Confinement effects on freezing and melting," *Journal of Physical Chemistry B,* vol. 107, pp. 6445-6453, 2003.

[56] S.-G. Jeong, J. Jeon, C. Junghoon, J. Kim and S. Kim, "Preparation and evaluation of thermal enhanced silica fume by incorporating organic PCM, for application to concrete,"

Energy and Buildings, vol. 62, pp. 190-195, 2013.

[57] C. Wang, L. Feng, W. Li, J. Zheng, W. Tian and X. Li, "Shape-stabilized phase change materials based on polyethylene glycol/porous carbon composite: The influence of the pore structure of the carbon materials," *Solar Energy Materials & Solar Cells,* vol. 105, pp. 21-26, 2012.

[58] C. Faivre, D. Bellet and G. Dolino, "Phase transitions of fluids confined in porous silicon: A differential calorimetry investigation," *The European Physical Journal B,* vol. 7, pp. 19-36, 1999.

[59] R. Radhakrishnan and K. E. Gubbins, "Free energy studies of freezing in slit pores: a order-parameter approach using Monte Carlo simulation," *Molecular Physics,* vol. 96, pp. 1249-1267, 1999.

[60] T.-C. Ling and C.-S. Poon, "Use of phase change materials for thermal energy storage in concrete: An overview," *Construction and Building Materials,* vol. 46, pp. 55-62, 2013.

[61] K.-H. Kim, S.-E. Jeon, J.-K. Kim and S. Yang, "An experimental study on thermal conductivity of concrete," *Cement and Concrete Research,* vol. 33, pp. 363-371, 2003.

[62] A. Sari and A. Karaipekli, "Thermal conductivity and latent heat thermal energy storage characteristics of paraffin/expanded graphite composite as phase change material," *Applied Thermal Engineering,* vol. 27, pp. 1271-1277, 2007.

[63] B. Xu and Z. Li, "Paraffin/diatomite composite phase change material incorporated cement-based composite for thermal energy storage," *Applied Energy,* vol. 105, pp. 229-237, 2013.

[64] Z. Sun, Y. Zhang, S. Zheng, Y. Park and R. L. Frost, "Preparation and thermal energy storage properties of paraffin/calcined diatomite composites as form-stable phase change materials," *Thermochimica Acta,* vol. 558, pp. 16-21, 2013.

[65] D. Ravikumar, M. Aguayo, A. Dakhane, J. Jain and N. Neithalath, "Microstructural, mechanical, and durability related similarities in structural concretes based on OPC and alkali activated slag binders".